The following publication Y. Zheng, M. Xu, S. Wu and S. Wang, "Maximum Platoon Size for Platoon-Based Cooperative Signal-Free Control at Intersections," in IEEE Transactions on Intelligent Transportation Systems, vol. 25, no. 12, pp. 20854-20871, Dec. 2024 is available at https://doi.org/10.1109/TITS.2024.3467213.

Maximum Platoon Size for Platoon-based Cooperative Signal-free Control at Intersections

Yuan Zheng, Min Xu*, Shining Wu, Shuaian Wang

***Abstract*—**Maximum platoon size (MPS) playing a crucial role in the configuration of connected and automated vehicle (CAV) platoons can significantly affect the traffic operation performance at intersections. The study addresses the MPS for platoon-based cooperative signal-free intersection control (PCSIC) problem considering the platoon formation process of the CAVs, which manage the CAVs to form the CAV platoons under the tactical platoon size limit to pass the intersection cooperatively. A mixed-integer nonlinear programming model is first developed to solve the proposed problem by minimizing the total travel delays of all CAVs while guaranteeing the feasible trajectories of the CAVs for platoon formation. A hybrid artificial bee colony algorithm integrating the artificial bee colony approach and dynamic programming algorithm for an optimal control scheme is proposed to solve the proposed model. Numerical experiments are conducted to examine the efficacy of the proposed model and solution algorithm. The impacts of balanced and unbalanced motion states between approaching directions on the MPS are investigated, and the traffic throughput performance of the platoon-based control strategy under balanced and unbalanced scenarios is evaluated. The findings can provide useful insights to transport authorities and automotive operators for signal-free intersection management.

***Key Words*—Connected and automated vehicles; signal-free intersection control; cooperative platoon control; platoon size; hybrid artificial bee colony algorithm.**

I. Introduction

In recent years, connected and automated vehicles (CAVs) have received considerable attention due to their benefits in improving traffic efficiency and reducing fuel consumption [1], [2], [3]. Notably, the CAVs can leverage the connectivity and platooning capabilities to form CAV platoons through advanced automation and vehicle-to-vehicle (V2V)/vehicle-to-infrastructure (V2I) communication technologies. This enables the CAVs to realize stable car-followings in a form of a string with a short inter-vehicle spacing for improving the performance of traffic operation [4], [5]. Moreover, many previous theoretical and experimental studies have proved the merits of CAV platoons in improving traffic throughput, reducing fuel consumption, and enhancing traffic flow stability [6], [7], [8].

Despite the noticeable benefits of vehicle platooning based on automatic control and real-time communication functionalities of CAVs, vehicle platooning technology creates new challenges for traffic management [9]. One of the prominent issues is autonomous intersection management in urban road networks, which is also called signal-free intersection management [10], [11]. Unlike the traditional traffic control strategies (e.g., fixed-time and real-time adaptive signal controls) for managing the traffic flow by a traffic signal [12], the signal-free intersection control can be implemented to safely and efficiently coordinate the movements of the CAVs and CAV platoons within the intersection without traffic signal [13], [14], which effectively addresses the drawbacks of traditional traffic signal control like clearance loss time for the traffic management at intersections [14], [15]. Therefore, the management and control of platooning for CAVs in the vicinity of intersections which improves the overall travel efficiency of all the CAVs passing the intersections, is of great practical significance for future CAV mobility.

A. Literature Review

In this subsection, we review the existing methods on the platoon formations of the CAVs and the recent studies on the CAV platoon-based cooperative control. The research gaps are identified after the literature review.

1) Platoon formation of CAVs

From a structural point of view, CAV platoon formation refers to the operation process of clustering the CAVs into a vehicular platoon according to the given operational decisions. For the realization of the platoon formation of CAVs, there are mainly three types of methods in the literature, i.e., simple motion planning [16], [17], linear/non-linear control [18], [19], and optimal control [20], [21]. The simple motion planning method includes three movement strategies, i.e., acceleration & cruise, deceleration & cruise, and cruise, which can be easily obtained by basic kinematics and require little computational cost. However, the simplified trajectories obtained by the method may not be smooth enough for the CAVs to form the platoons in practice, due to speed jumps or excessive acceleration and deceleration movements. The linear/non-

Yuan Zheng is with the School of Transportation, Southeast University, Nanjing, China; Jiangsu Province Collaborative Innovation Center of Modern Urban Traffic Technologies, Nanjing, China; Jiangsu Key Laboratory of Urban ITS, Nanjing, China. (Email: 101013486@seu.edu.cn)

Min Xu* is with the Department of Industrial and Systems Engineering, The Hong Kong Polytechnic University, Hung Hom, Hong Kong. (Email: xumincee@gmail.com; min.m.xu@polyu.edu.hk)

Shining Wu and Shuaian Wang are with the Department of Logistics & Maritime Studies, The Hong Kong Polytechnic University, Hong Kong.

linear control method is a distributed adaptive control model that allows the CAVs to implement real-time control of movements based on the collected state information of predecessors using the linear/non-linear feedback controllers. With this method, the CAVs can adjust the movements iteratively to form the platoons based on the collected state information. For example, a gap-closing linear feedback controller was proposed to facilitate the following CAVs to catch up with the preceding CAV for grouping into a platoon by adjusting the controller gain parameters [19]. Moreover, some studies have been devoted to the platoon control of CAVs based on linear/non-linear control methods. For example, Zheng et al. (2016) explored the impacts of information flow topology on the internal stability and scalability of homogeneous CAV platoons [22]. The stabilizing thresholds of linear controller gains for platoons under different information flow topologies were derived based on the algebraic graph theory and Routh–Hurwitz stability criterion. Liu et al. (2022) developed a distributed cooperative compound tracking control method based on backstepping, an adaptive neural network, and designed prescribed performance control, in which the adaptive neural network and backstepping method were utilized for achieving distributed cooperative regulation [23]. Numerical experiments were conducted to verify the effectiveness in ensuring practical finite-time stability and asymptotical convergence. Liu et al. (2023) proposed a distributed adaptive fixed-time platoon tracking problem for heterogeneous nonlinear vehicles based on the third-order modified dynamics and distributed nonlinear fixed-time tracking algorithm [24]. Yu et al. (2023) developed a distributed data-driven model predictive control strategy by combining the data-driven model with the distributed model predictive control algorithm [25]. The data-driven model with subspace identification can be established based on the input-output vehicle trajectory. Moreover, the recursive feasibility and exponential stability were proved by an input/output-to-state stability Lyapunov function and an optimal sum cost function. Although the linear/non-linear control method is easy to be implemented in practice, it cannot guarantee the efficiency of the platoon formation by multiple CAVs. Moreover, the collision-free constraint within a reasonable acceleration/ deceleration limit cannot explicitly be formulated into the control model, which cannot ensure safety during the platoon formation process [4].

Unlike the above two methods, the optimal control method is a kind of optimization control model, which determines the optimal control input over a time horizon given the initial motion states and system dynamics model while incorporating the key constraints, such as the bounded acceleration/ deceleration and collision avoidance. The trajectory design of the platoon formation involving multiple CAVs can be formulated as the optimal control problem. As a result, the trajectories of the CAVs for platoon formation during a certain predictive time horizon can be obtained by solving the constrained optimal control model. For example, an optimal control model was developed to determine the optimal trajectories of CAVs to form a platoon that minimized the total fuel consumption of the CAVs given the vehicle sequence [26]. The dynamic programming algorithm was applied to solve the optimal trajectories. Numerical experiments were conducted to validate that the total fuel consumption during the platoon formation process can be reduced by following the optimal CAV trajectories obtained by the proposed model in contrast to that of the benchmark model. Compared with the aforementioned simple motion planning and linear/non-linear feedback control methods, the optimal control method can utilize the received system-wide motion state information and provide the optimal CAV trajectories for platoon formation, through coordinated movements of the involved CAVs while respecting the collision-free and acceleration/deceleration constraints. However, the computational efficiency to obtain the CAV trajectories for platoon formation can decrease as the number of CAVs increases. Nevertheless, some solution algorithms such as dynamic programming and Pontryagin's minimum principle-based have been proposed to reduce solution time [27], [28].

2) CAV platoon-based cooperative control

As motivated by the emerging CAV and vehicle platooning technologies [7], [14], [29], some recent studies have been devoted to CAV platoon-based cooperative signal-free control to improve traffic performance at intersections [15], [30], [31], [32], which are summarized in Table I. For example, Bashiri et al. (2018) investigated the optimal passing sequence of the CAV platoons traversing the intersection for autonomous intersection management [30]. An optimization model was formulated to determine the best sequence for the CAV platoons that minimized the total travel delays and delay variances of all the CAVs. Given the obtained passing sequence, the linear controller was adopted to allow the CAVs to form the platoons for passing the intersection. The results from numerical experiments verified the effectiveness of the proposed platoon-based signal-free control in improving intersection throughput and fuel consumption against traditional signal control and the positive impacts of platoon size on the throughput and fuel consumption. Cristofoli (2019) built an optimization model to determine the optimal sequence and acceleration profiles with the least total travel delays for the vehicle platoons to pass the intersection, in which the vehicle platoons can be grouped by a batch of vehicles with headways less than the threshold [31]. The solution algorithm integrating the branching and simple motion planning methods was developed to solve the model. Numerical results demonstrated that the proposed control strategy could improve travel efficiency at the intersection compared with the benchmark strategy. Zhao et al. (2021) studied the joint optimization problem of platoon-based intersection control and trajectory planning by developing a bi-level programming model [32]. The upper-level and lower-level models were to determine the passing sequence and assigned time to the intersection by minimizing the total travel delays and to determine the speed profiles by maximizing the total speeds of all the CAVs entering the intersection, respectively. The platoon-based customized heuristic algorithm was developed to solve the proposed model. The results indicated that the proposed bi-level model could perform better in terms of average delay and throughput than the benchmark model with no feedback between the upper and lower models. It implied that the lower-level trajectory planning had a significant

impact on the upper-level decisions of passing sequence and assigned time. In addition, some studies used the virtual platoon control method to coordinate the trajectories of the CAVs to traverse the intersections for signal-free intersection management [33]. It can be implemented by mapping two-dimension vehicle movements to a one-dimension virtual platoon according to a specific rule like First-Input-First-Output, and thus the CAVs can be organized into the coordinated independent virtual platoons with the multiple vehicle communication topology. For example, Zhou et al. (2022) proposed a distributed adaptive sliding controller based on the customized communication tolopoly [15]. With the proposed controller, the CAVs grouped into the same virtual platoons can follow the reference speed and maintain the desired safe spacing with guaranteed stability under parametric inaccuracies and vehicle dynamics disturbances so as to improve travel efficiency at intersections.

The highway CAV platoon-based cooperative merging control for the on-ramp scenarios is analogous to the CAV platoon-based cooperative signal-free intersection control [16], [17], [20]. Xu et al. (2019) investigated the passing sequence problem for the cooperative driving between mainline and on-ramp CAV platoons, where the CAVs can be clustered into the same platoon if the headways were smaller than a grouping threshold [17]. A grouping rule-based strategy was proposed to find the near-optimal passing sequence by minimizing the total travel delays and maximum assigned time of all the CAVs. For simplification, the assigned times were obtained by the simple motion planning method. Ding et al. developed a rule-based two-stage model to determine the passing sequence, assigned time, and acceleration profiles for the platoon-based cooperative merging at the highway on-ramp [16]. The first-stage model was to determine the near-optimal sequence and assigned time that minimized the total travel delays of the involved CAVs to the merging zone using the proposed rule-adjusted algorithm. Given the obtained passing sequence, the second-stage model was to calculate the trajectories of the leader using the optimal control method and the trajectories of followers grouped into the platoons using the linear control method. As indicated by the results, the proposed platoon-based control strategy could have better performance in throughput and delay compared with the benchmark vehicle-based control strategy. Duret et al. (2020) addressed the splitting of mainline CAV platoons to facilitate the efficient and safe merging of the on-ramp vehicles by developing an optimization control approach with the two layers [20]. The upper-layer can maximize the traffic flow at the on-ramp to determine the optimal vehicle orders after the merge and the assigned times that the vehicles in the platoon actively created the gaps for the merging vehicles. The lower-layer used the optimal control method to calculate the optimal trajectories to the highway merging point based on the inter-vehicle desired time gaps as commanded by the upper-layer. Numerical experiments demonstrated the feasibility and effectiveness of the proposed control approach.

Based on the existing literature, we can see that most studies focused on determining the passing sequence, assigned time, and trajectory planning of the CAV platoons to the intersection conflict zones and highway merging zones for platoon-based cooperative signal-free and merging controls. So far, no one has paid attention to optimizing tactical decisions such as MPS, which may largely affect the overall travel efficiency at intersections. Intuitively, a large-size CAV platoon can be beneficial to improve the travel efficiency of the current approaching direction at intersections. However, the travel efficiency of other conflicting directions can be negatively affected by the adoption of large platoon size. In addition, lots of research efforts have been made to first determine the passing sequence and assigned time and then the trajectories of the CAVs for platoon formation based on the two-stage/two-layer models. The impacts of CAV trajectories for platoon formation on the passing sequence and assigned time have been rarely considered for the simplification of modeling. Although a few studies have jointly optimized both the passing sequence and assigned time and the CAV trajectories forming the platoons for the PCSIC problem, the obtained trajectories by the simple motion planning methods may not be applied to the practical formation of CAV platoons.

Table I Summaries of CAV platoon-based cooperative control.

Methods	Upper model	Lower model	Interaction	Platoon formation process
Bashiri et al. (2018)	Optimization model of minimizing the total travel delays and delay variances	Linear controller for CAV trajectories	×	×
Cristofoli (2019)	Optimization model of minimizing the total travel delays	Simple motion planning for CAV trajectories	×	×
Zhao et al. (2021)	Optimization model of minimizing the total travel delays	Trajectory planning method for CAV trajectories	√	×
Zhou et al. (2022)	/	Distributed adaptive sliding controller for CAV trajectories	×	×
Xu et al. (2019)	Optimization model of minimizing the total travel delays	Simple motion planning for CAV trajectories	×	×
Ding et al. (2020)	Optimization model of minimizing the total travel delays	Optimal control and linear control for CAV trajectories	×	×
Duret et al. (2020)	Optimization model of maximizing the traffic flows	Optimal control for CAV trajectories	×	×
Our study	Optimization model of minimizing the total travel delays	Optimal control for CAV trajectories	√	√

B. Objectives and Contributions

To close the gaps, the study investigates the MPS for the PCSIC problem considering the platoon formation process of the CAVs in the vicinity of intersections. The objective of the study is to minimize total travel delays of all the CAVs by determining the optimal tactical platoon size threshold while considering the operational decisions, i.e., formation pattern, passing sequence, and assigned time of CAV platoons to the intersection conflict point as well as the CAV trajectories for platoon formation. To achieve the objective, a novel mixed-integer nonlinear programming (MINLP) model is formulated by explicitly incorporating the platoon size limit and the CAV trajectories for platoon formation constraints. Due to the complex formation process of the CAV platoons considered in

the proposed model, the proposed model cannot be easily solved by commercial solvers. Therefore, we design a hybrid artificial bee colony algorithm integrating the artificial bee colony approach and dynamic programming algorithm for an optimal control scheme to obtain good-quality solutions. Numerical experiments are carried out to verify the effectiveness of the proposed model and solution algorithm. We also analyze the balanced and unbalanced motion states between approaching directions on the MPS and the traffic performance of the platoon-based control strategy in terms of travel delay and throughput.

The contributions of our study are presented as follows:

(1) We first proposed a bi-level platoon-based signal-free intersection control model that combines the optimization management and optimal control schemes in the model considering the platoon formation process of CAVs, in which the upper-level model is to determine the formation pattern, maximum platoon size, passing sequence, and assigned time of CAV platoons, and the lower-level is to determine the optimal trajectories of CAVs for platoon formation;

(2) We develop a customized hybrid artificial bee colony algorithm integrating the artificial bee colony approach and dynamic programming algorithm for an optimal control scheme to solve the proposed model, which fully takes advantage of the merits of the two algorithms;

(3) The changes in the maximum platoon sizes for platoon-based control strategy and its impacts on traffic operation performances under the balanced and unbalanced motion states between approaching directions are investigated. The better traffic throughput performances of the proposed platoon-based control strategy are also verified compared with the baseline strategy.

The remainder of this study is organized as follows. Section 2 presents the assumptions, notations, and problem description. Section 3 formulates the optimization model for the platoon-based cooperative signal-free intersection control. Section 4 introduces the solution algorithm for the proposed model. Section 5 elaborates on the case studies and experimental results in detail and Section 6 presents the discussion. Section 7 concludes this study with future research directions.

II. PROBLEM DESCRIPTION

Consider an intersection within a control zone illustrated in Fig. 1(a) (see the circle area within the orange dashed curve). Let $\boldsymbol{Z}$ denote the set of all the approaching directions at the intersection and $\boldsymbol{I}_z$ be the set of CAVs of our interest in the direction $z \in \boldsymbol{Z}$. The time instant when the most leading vehicle in the zone (e.g., CAV_1 in Fig. 1(a)) reaches the decision location of its direction is denoted by t^0. We will study all the scattered CAVs located between the pre-specified decision location (see the yellow line in Fig. 1(a)) and the boundary of the control zone in the vicinity of the intersection at the time instant t^0.

We assume that all the CAVs within the control zone can exchange real-time motion information, i.e., position, speed, and acceleration, with one another and share the information with a signal-free intersection controller via V2V and V2I communications. The CAVs in each direction can form CAV platoons with different platoon sizes to traverse the intersection.

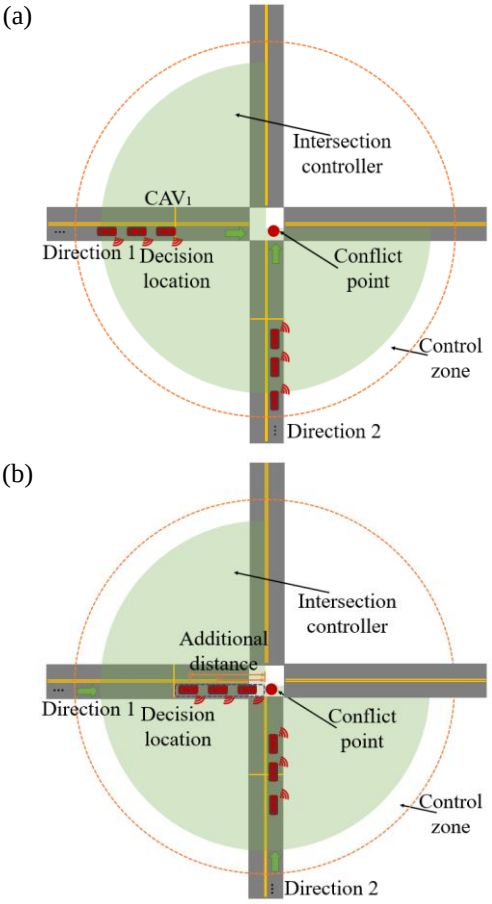

Fig. 1. Illustration of two streams of cross-moving CAVs at the intersection: (a) at the time t^0; (b) at the time t_z^{k*}

Without loss of generality, we assume that the movement formation of CAV platoons in the control zone follows the optimal control scheme and the over-taking of CAVs for the platoon formations is not allowed. Specifically, let $\boldsymbol{I}_z^k$ be the set of CAVs in the *k*th platoon formed of direction *z*. Kindly note that a travel-alone CAV can be viewed as a platoon of size 1, and thus we have $k \le |\boldsymbol{I}_z|$. Let $p_i(t)$, $v_i(t)$, and $u_i(t)$ represent the front bumper position, speed, and control input (i.e., acceleration prescribed by vehicle controller) of CAVs for $i \in \boldsymbol{I}_z^k$ at time t respectively. Let $\boldsymbol{u}_z^k(t)$ and $\boldsymbol{x}_z^k(t) = \left[\boldsymbol{p}_z^k(t)^T, \boldsymbol{v}_z^k(t)^T\right]^T$ denote the acceleration and state column vector of the *k*th platoon in direction *z* at time *t*, respectively, where $\boldsymbol{p}_z^k(t)$ and $\boldsymbol{v}_z^k(t)$ denote the position and speed column vector of the *k*th platoon in direction *z* at time *t*, respectively. The optimal control scheme of the *k*th platoon in direction *z* is essentially to determine the optimal acceleration and state sequences (namely the acceleration and state trajectories) of all CAVs in set $\boldsymbol{I}_z^k$ for platoon formations over the assigned time horizon $\left[t^0, t_z^k\right]$ by minimizing a performance index denoted by *J* to be elaborated later. For ease

of model formulation, we define the terminal performance measures $\left\{\tilde{p}_z^k, \tilde{d}_z^k, \tilde{v}_z^k\right\}$ of a platoon formed by CAVs in set $\boldsymbol{I}_z^k$ at time t_z^k, where $\tilde{p}_z^k$ denotes the terminal position of a platoon represented by the terminal position of the first CAV in the platoon, $\tilde{d}_z^k$ denotes the terminal headway of a platoon obtained by averaging the terminal headways of the following CAVs in the platoon, and $\tilde{v}_z^k$ denotes the terminal speed of a platoon by averaging the average terminal speeds of the CAVs in the platoon. For simplicity, we assume the formations of the CAV platoons will be completed at the conflict point (denoted by $\hat{p}$, see the red dot in Fig. 1(a)), with the pre-specified terminal headway (denoted by $\hat{d}$), and terminal speed (denoted by $\hat{v}$), for $\forall z \in \boldsymbol{Z}, k = 1,2,...,\left|\boldsymbol{I}_z\right|$ at the assigned time t_z^k, where the conflict point is viewed as the pre-specified terminal position. Ideally, the terminal position, headway, and speed measures of a CAV platoon would be the same as the pre-specified terminal ones accordingly.

Given the motion state information of all the CAVs in the set $\bigcup_{z\in\boldsymbol{Z}} \boldsymbol{I}_z$ at the time t^0, i.e., $p_i(t^0)$ and $v_i(t^0)$ for $\forall i \in \bigcup_{z\in\boldsymbol{Z}} \boldsymbol{I}_z$, the intersection controller will determine (1) the optimal formation patterns of the platoons in each direction (e.g., the index of the CAVs grouped into the *k*th platoon of direction *z*, i.e., $\boldsymbol{I}_z^{k*}$); (2) the passing sequence of the platoons traversing the conflict point; (3) the assigned time of the platoons reaching the conflict point (e.g., the assigned time of the *k*th platoon in direction *z*, i.e., t_z^{k*}); (4) the maximum platoon size of the platoons in the direction *z*, i.e., c_z^*; (5) ultimately the acceleration and state trajectories of each CAV to form the platoons according to the formation patterns while traversing the conflict point following the passing sequence and assigned time (e.g., the values of $u_i^*(t)$ for $\forall t \in \left[t^0, t_z^{k*}\right), i \in \boldsymbol{I}_z^{k*}$ and the values of $p_i^*(t)$ and $v_i^*(t)$ for $\forall t \in \left(t^0, t_z^{k*}\right], i \in \boldsymbol{I}_z^{k*}$). The objective of this study is to minimize the total travel delays of all the CAVs by determining the tactical platoon size threshold in each approaching direction while considering the aforementioned operational decisions.

A. Optimal control for platoon formation of CAVs

Regarding the optimal control scheme for platoon formation of CAVs, the control model is represented by the total cost function during the platoon formation process. Given the formation patterns (i.e., $\boldsymbol{I}_z^{k*}$), initial state of the CAVs (i.e., $\boldsymbol{p}_z^{k*}(t^0)$ and $\boldsymbol{v}_z^{k*}(t^0)$), and assigned time (i.e., t_z^{k*}) of the *k*th platoon in direction *z*, as well the CAV position trajectories of the preceding platoon (i.e., $\boldsymbol{p}_z^{(k-1)*}$ consisting of $p_i^*(t)$ for $\forall t \in \left[t^0, t_z^{(k-1)*}\right], i \in \boldsymbol{I}_z^{(k-1)*}$) and the pre-specified terminal performance measures (i.e., $\hat{p}$, $\hat{d}$, and $\hat{v}$), the optimal acceleration and state trajectories of the CAVs for the formation of the *k*th platoon in direction *z* during the time horizon $\left[t^0, t_z^{k*}\right]$, denoted by $\left[OC_z^k\right]$, can be determined by solving the following model:

$$\left[OC_z^k\right] \min_{\boldsymbol{x}_z^k, \boldsymbol{u}_z^k} J = \int_{t^0}^{t_z^{k*}} \mathcal{L}\left(\boldsymbol{x}_z^k(t), \boldsymbol{u}_z^k(t)\right) dt + \zeta\left(\boldsymbol{x}_z^k(t_z^{k*})\right) \quad (1)$$

subject to

$$\dot{\boldsymbol{x}}_z^k(t) = \boldsymbol{A}\boldsymbol{x}_z^k(t) + \boldsymbol{B}\boldsymbol{u}_z^k(t), \forall z \in \boldsymbol{Z}, k = 1,2,...,\left|\boldsymbol{I}_z\right|, t \in \left[t^0, t_z^{k*}\right] \quad (2)$$

$$v_{\min} \le v_i(t) \le v_{\max}, \forall i \in \boldsymbol{I}_z^{k*}, t \in \left[t^0, t_z^{k*}\right] \quad (3)$$

$$u_{\min} \le u_i(t) \le u_{\max}, \forall i \in \boldsymbol{I}_z^{k*}, t \in \left[t^0, t_z^{k*}\right) \quad (4)$$

$$p_j^*(t) - p_i(t) \ge L, \forall j \in \boldsymbol{I}_z^{(k-1)*}, i \in \boldsymbol{I}_z^{k*}, t \in \left[t^0, t_z^{k*}\right] \quad (5)$$

$$p_{i^-}(t) - p_i(t) \ge L, \forall t \in \left[t^0, t_z^{k*}\right], i \in \boldsymbol{I}_z^{k*} \quad (6)$$

$$\left|p_i(t_0) - \hat{p}\right| < D_c, \forall i \in \boldsymbol{I}_z^{k*} \quad (7)$$

where *J* denotes the total cost consisting of the running cost $\mathcal{L}$ and the terminal cost ζ (introduced in section 4), matrix $\boldsymbol{A}^{2n\times 2n} = \begin{bmatrix} \boldsymbol{0} & \bar{\boldsymbol{A}} \\ \boldsymbol{0} & \boldsymbol{0} \end{bmatrix}$, $\boldsymbol{B}^{2n\times 1} = \begin{bmatrix} \boldsymbol{0} \\ \bar{\boldsymbol{B}} \end{bmatrix}$, $\bar{\boldsymbol{A}}^{n\times n} = \begin{bmatrix} 1 & & \\ & \ddots & \\ & & 1 \end{bmatrix}$, $\bar{\boldsymbol{B}}^{n\times 1} = \begin{bmatrix} 1 \\ \vdots \\ 1 \end{bmatrix}$ where $n = \left|\boldsymbol{I}_z^{k*}\right|$, *L* is the safety buffer distance, $v_{\min}$ and $v_{\max}$ are the upper and lower bounds of speed, respectively, $u_{\min}$ and $u_{\max}$ are the minimum and maximum acceleration, respectively, and D_c is the length of the control zone. Constraint (2) represents the system dynamics of CAV platoons. Constraints (3) and (4) ensure the acceleration and speed within the reasonable range of $\left[v_{\min}, v_{\max}\right]$ and $\left[u_{\min}, u_{\max}\right]$ at any time instant over the time horizon, respectively. Constraint (5) restricts that the actual spacing between vehicle *j* in the (*k*-1)th platoon and vehicle *i* in the *k*th platoon in the same direction *z* maintains the safety buffer distance. Constraint (6) guarantees that the actual spacing between two consecutive CAVs in the same platoon is no smaller than the safety buffer distance, where i^- is the index of the immediate predecessor of vehicle *i* in the set $\boldsymbol{I}_z^{k*}$. Constraint (7) ensure information transmission of all CAVs in the control zone.

Kindly note that the CAV trajectories obtained by the aforementioned model $\left[OC_z^k\right]$ may be undesired for platoon formation due to unfeasible decisions (e.g., too small assigned time). In other words, the output terminal performance measures (i.e., terminal position, headway, and speed) for the trajectories of a CAV platoon can largely deviate from the pre-specified terminal performance measures under the unfeasible decisions. In addition to the acceleration and state trajectories during the assigned time horizon of the CAVs for platoon formations, we need to further output the terminal performance measures of the CAV platoons and the additional times of CAVs in the platoons. Based on the obtained acceleration and

state trajectories, we can calculate the optimal terminal performance measures of the platoons (e.g., the values of $\tilde{p}_z^{k*}$, $\tilde{d}_z^{k*}$, and $\tilde{v}_z^{k*}$ of the *k*th platoon in direction *z*), and CAV additional time column vector of the platoons to travel the additional distance (see the orange line in Fig. 1(b)) between the position at time t_z^{k*} to the conflict point at a constant speed (e.g., the vector of the *k*th platoon in direction *z*, i.e., $\tilde{\boldsymbol{t}}_z^{k*}$). Therefore, the output set $\boldsymbol{\Psi}$ and return set $\tilde{\boldsymbol{\Psi}}$ of the model $\left[OC_z^k\right]$ are presented as follows:

$$\begin{aligned}\boldsymbol{\Psi}(\boldsymbol{x}_z^{k*},\boldsymbol{u}_z^{k*}) &= \arg\min J\left(\boldsymbol{I}_z^{k*},t_z^{k*},t^0,\hat{p},\hat{d},\hat{v},\boldsymbol{p}_z^{k*}(t^0),\boldsymbol{v}_z^{k*}(t^0),\boldsymbol{p}_z^{(k-1)*}\right),\forall z\in\boldsymbol{Z},k=2,...,|\boldsymbol{I}_z| \\ \tilde{\boldsymbol{\Psi}}(\tilde{p}_z^{k*},\tilde{d}_z^{k*},\tilde{v}_z^{k*},\tilde{\boldsymbol{t}}_z^{k*}) &\Leftarrow \boldsymbol{\Psi}(\boldsymbol{x}_z^{k*},\boldsymbol{u}_z^{k*}),\forall z\in\boldsymbol{Z},k=2,...,|\boldsymbol{I}_z|\end{aligned} \quad (8)$$

III. Model Formulation

Let y_z^k denote a binary variable, $y_z^k=1$ if the *k*th platoon in direction *z* is a not null CAV platoon, and $y_z^k=0$ otherwise. Let w_{zi}^k denote a binary variable, $w_{zi}^k=1$ if vehicle *i* joins the *k*th platoon in direction *z*, and $w_{zi}^k=0$ otherwise. Let $\tilde{t}_{zi}^{k*}$ represent the additional time of vehicle *i* in the *k*th platoon of direction *z* required to travel the additional distance between its position at time t_z^{k*} to the conflict point. Let $\overline{t}_i$ represent the minimum travel time of vehicle *i* in direction *z* required to reach the conflict point. Note that the minimum travel time can be calculated based on the basic kinematics under the case where each CAV individually moves toward the conflict point first accelerating to the pre-specified terminal speed and then cruising. With above the notations, the total travel delays of all the CAVs will be calculated by

$$T=\sum_{z\in\boldsymbol{Z}}\sum_{k=1}^{|\boldsymbol{I}_z|}\sum_{i\in\boldsymbol{I}_z}(t_z^k y_z^k+\tilde{t}_{zi}^{k*}w_{zi}^k y_z^k-\overline{t}_i w_{zi}^k y_z^k) \quad (9)$$

Moreover, the total errors between the output and pre-specified terminal performance measures of the CAV platoons in all approaching directions will be calculated by

$$E=\sum_{z\in\boldsymbol{Z}}\sum_{k=1}^{|\boldsymbol{I}_z|}\left(\left|\tilde{p}_z^{k*}-\hat{p}\right|+\left|\tilde{d}_z^{k*}-\hat{d}\right|+\left|\tilde{v}_z^{k*}-\hat{v}\right|\right)y_z^k \quad (10)$$

To ensure the trajectory feasibility of the CAVs to form the platoons with the least total travel delays while traversing the conflict point and reaching the pre-specified headway and speed, the total errors of the terminal performance measures of all CAV platoons are designed as a penalty term and added to the objective function. The MPS for PCSIC at intersections problem can be formulated by the following model:

$$[\text{PCSIC}]\ \min_{\mathbf{w},\mathbf{y},\mathbf{c},\mathbf{s},\mathbf{t},\mathbf{x},\mathbf{u}}\ OBJ(\mathbf{w},\mathbf{y},\mathbf{c},\mathbf{s},\mathbf{t},\mathbf{x},\mathbf{u})=T+M\times E \quad (11)$$

subject to (2), (3), (4), (5), (6), (8) and

$$\sum_{k=1}^{|\boldsymbol{I}_z|}w_{zi}^k=1,\forall z\in\boldsymbol{Z},i\in\boldsymbol{I}_z \quad (12)$$

$$M\sum_{i\in\boldsymbol{I}_z}w_{zi}^{k-1}\geq\sum_{i\in\boldsymbol{I}_z}w_{zi}^k,\forall z\in\boldsymbol{Z},k=2,3,...,|\boldsymbol{I}_z| \quad (13)$$

$$y_z^k\leq\sum_{i\in\boldsymbol{I}_z}w_{zi}^k\leq My_z^k,\forall z\in\boldsymbol{Z},k=1,2,...,|\boldsymbol{I}_z| \quad (14)$$

$$\sum_{k'=1}^{k}w_{zi^-}^{k'}\geq w_{zi}^k,\forall z\in\boldsymbol{Z},k=1,2,...,|\boldsymbol{I}_z|,i\in\boldsymbol{I}_z \quad (15)$$

$$\sum_{i\in\boldsymbol{I}_z}w_{zi}^k\leq c_z,\forall z\in\boldsymbol{Z},k=1,2,...,|\boldsymbol{I}_z| \quad (16)$$

$$t_z^{k+1}-t_z^k\geq\sum_{i\in\boldsymbol{I}_z}w_{zi}^k(\hat{d}+L)/\hat{v},\forall z\in\boldsymbol{Z},k=1,2,...,|\boldsymbol{I}_z|-1 \quad (17)$$

$$t_z^k-t_{z'}^{k'}+Ms_{kk'}\geq\sum_{i\in\boldsymbol{I}_{z'}}w_{z'i}^{k'}(\hat{d}+L)/\hat{v},\forall z\in\boldsymbol{Z},z'\in\boldsymbol{Z}\setminus\{z\},k=1,2,...,|\boldsymbol{I}_z|,k'=1,2,...,|\boldsymbol{I}_{z'}| \quad (18)$$

$$w_{zi}^k\in\{0,1\},\forall z\in\boldsymbol{Z},i\in\boldsymbol{I}_z,k=1,2,...,|\boldsymbol{I}_z| \quad (19)$$

$$y_z^k\in\{0,1\},\forall z\in\boldsymbol{Z},k=1,2,...,|\boldsymbol{I}_z| \quad (20)$$

$$s_{kk'}\in\{0,1\},\forall z\in\boldsymbol{Z},z'\in\boldsymbol{Z}\setminus\{z\},k=1,2,...,|\boldsymbol{I}_z|,k'=1,2,...,|\boldsymbol{I}_{z'}| \quad (21)$$

$$c_z\in\mathbb{Z}^+,\forall z\in\boldsymbol{Z} \quad (22)$$

$$t_z^k\in\mathbb{R}^+,\forall z\in\boldsymbol{Z},k=1,2,...,|\boldsymbol{I}_z| \quad (23)$$

where i^- is the index of the predecessors of vehicle *i* in the *k*th platoon of the direction *z*, the decision variable $c_z,\forall z\in\boldsymbol{Z}$ denotes the maximum allowable vehicle number in a CAV platoon of the direction *z*, $s_{kk'},\forall z\in\boldsymbol{Z},z'\in\boldsymbol{Z}\setminus\{z\},k=1,2,...,|\boldsymbol{I}_z|,k'=1,2,...,|\boldsymbol{I}_{z'}|$ is a binary variable for determining the passing sequence between the CAV platoons in different directions, $s_{kk'}=1$ if the *k*th platoon in the direction *z* has the right of priority over the k'th platoon in the direction z', and *M* is a large positive constant.

The objective function in Eq. (11) is the sum of the total travel delays of all the CAVs and a big-*M* component. Since our study aims to manage and control the CAVs to form the platoons while traversing the conflict point and reaching the pre-specified headway and speed, the unfeasible CAV trajectories are penalized by the big-*M* component in the objective function. Constraint (12) ensures that each CAV joins a CAV platoon. Constraints (13) and (14) ensures that the CAV platoons can be continuously formed. Constraint (15) guarantees that no overtaking of CAVs for platoon formation can occur. Constraint (16) restricts that the total number of CAVs in a platoon cannot exceed the upper bound of platoon size. Constraints (17) and (18) ensure that the difference in the assigned time to the conflict point between the two CAV platoons from the same direction or one from a different direction is maintained no smaller than the summation of the time headway (namely the sum of the pre-specified terminal and safety distance divided by the pre-specified terminal speed)of each CAV in the preceding CAV platoon. Constraints (19), (20), (21), (22), and (23) define the domains of variables w_{zi}^k, y_z^k, $s_{kk'}$, C_z, and t_z^k.

IV. Solution Algorithm

Due to the complex formation process of the CAV platoons, the CAV trajectories for platoon formation with a restriction of the pre-specified terminal performance measures cannot be directly expressed in the proposed model [PCSIC]. Therefore, the trajectories of the CAVs for platoon formation are taken as a constraint of the proposed model [PCSIC], which is represented by the optimal control model $\left[OC_z^k\right]$. The

consideration of the CAV trajectories for platoon formation leads to a non-linear model that cannot be easily solved by commercial solvers. Moreover, we can see that when the formation pattern, passing sequence, and assigned time of a CAV platoon to the intersection conflict point, and the initial input information of a platoon are given, the proposed model [PCSIC] reduces to the model $\left[OC_z^k\right]$. The model $\left[OC_z^k\right]$ can be efficiently solved by the dynamic programming algorithm for an optimal control scheme. This is because the dynamic programming algorithm has shown good computation efficiency and convergence accuracy in solving the trajectories of the CAV platoons under the optimal control schemes [34]. To obtain the optimal formation patterns, passing sequence, and assigned time of the CAV platoons, we need an efficient search algorithm that updates these operational decisions in each iteration. There are some heuristic algorithms such as genetic algorithm and artificial bee colony (ABC) for solving the optimization problems with non-linear models, among which the ABC algorithm proposed by [35] shows a better iterative search mechanism and can accelerate convergence to a high-quality solution. The ABC algorithm has been widely applied to solve optimization problems in the transportation field in recent years, such as vehicle routing and ride-hailing problems [36], [37]. Therefore, we develop a novel solution algorithm integrating the ABC approach and dynamic programming algorithm for an optimal control scheme, referred as to the hybrid ABC algorithm in the rest of the paper, to solve the proposed model [PCSIC].

In what follows, we first introduce the overall procedures of the proposed hybrid ABC algorithm. Moreover, we illustrate the key modules of the proposed algorithm, including solution representation, solution initialization and renewal, neighborhood operator, selection of solution sources, and dynamic programming algorithm to solve the model $\left[OC_z^k\right]$.

A. Overview of hybrid ABC algorithm solve model [PCSIC]

In this subsection, the overviews of the basic ABC algorithm and hybrid ABC algorithm will be presented, respectively.

1) Basic ABC algorithm

ABC is an optimization algorithm based on the intelligent behaviors of honey bees in searching for food sources in the vicinity of the hives. In the ABC algorithm, the colony of artificial bees is divided into employed bee, onlooker bee, and scout bee. The employed bees are responsible for searching for food sources, in which each employed bee is associated with one and only one food source. The employed bees can gather the required information on the food sources and share the information with onlooker bees. The onlooker bees then probabilistically select a food source among the food sources found by the employed bees, in which a more profitable food source would be chosen with a higher probability. The employed bee becomes a scout and exploits a new food source in the vicinity of the hive, when it cannot find a better food source after executing a maximum number of iterations.

For the application of the ABC algorithm to solve the optimization problem, the food source represents the solution to the optimization problem, and the nectar count of the food source corresponds to the objective values or fitness of the solutions. At the start, the ABC algorithm, as a swam-based heuristic algorithm, generates the random solutions as the initial food sources and assigns each employed bee to a food source. During each iteration, the employed bee exploits the new food source near the current source using the neighborhood operator, and the nectar count of the new food sources found is then evaluated. If the nectar count of the new food source is larger than the old one, the employed bee can be assigned to the new one, and the old one is abandoned. After all the employed bees finish the exploited process, they will share the nectar count information with the onlooker bees. The onlooker bees can select the food sources according to the shared information from the employed bees using a roulette wheel selection method. Meanwhile, the onlooker bee can also search for new food sources near its selected source using the neighborhood operator and further assess the nectar count of the new food source. The best new food source can be determined by the greedy method. If the new food source has more nectar count than the old one, the old one will be abandoned and replaced by the new one. The employed bee can be allocated to the best new food source. In addition, the nectar count of the food source has been not improved under the limited iterations, i.e., a pre-determined limit, and the employed bee will become a scout bee, and the food source will be abandoned with a new one. The scout bee starts to randomly find a new food source, and it becomes an employed bee again after a new food source is found. Afterward, the iteration of the ABC algorithm will update after the three groups of bees have completed the search tasks. The whole process is repeated to search for the best solution until the terminal conditions are satisfied.

2) Hybrid ABC algorithm

The flow diagram of the proposed hybrid ABC algorithm jointly formulated by the ABC algorithm and dynamic programming algorithm is illustrated in Fig. 2. For the ABC algorithm in the proposed method with the maximum number of iterations N_m, a population of initial solutions is generated by the employed bees in the initiation phase. Each employed bee is responsible for one randomly generated solution. The procedures of the employed bee and onlooker bee phases are similar. The difference between the two phases lies in the rule of selecting the candidate solution for a neighborhood search. In the respective phase, each employed bee selects its associated solution and each onlooker bee selects a solution based on the fitness value. Both two phases utilize the dynamic programming algorithm to determine the CAV trajectories to form the platoons, additional times required by CAVs in the platoons, and terminal performance measures of the platoons under the given formation patterns, passing sequence, and assigned time of the CAV platoons for each solution in each iteration. Based on this, the fitness value of each solution can be calculated in each iteration. Afterward, the greedy selection strategy is conducted for the two phases after evaluating the fitness value of the new solution. If the new solution is better than the old solution, the new one can replace the old one, and its limit value is set to 0. Otherwise, the old one is kept and the limit value is increased by 1. The employed bee and onlooker bee phases are terminated after all the employed bees and

onlooker bees complete the neighborhood research, respectively. In the scout bee phase, all the solutions are scanned and a solution that cannot be improved under the limit of successive iterations is abandoned and replaced by a randomly generated new solution.

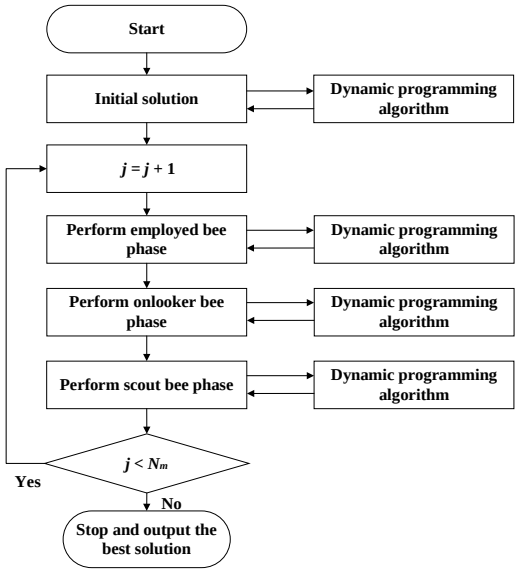

Fig. 2. Flow diagram of the hybrid ABC algorithm

B. Solution representation

The solution (food source) of the proposed hybrid ABC algorithm can present the decision information of CAV platoons including the formation pattern, passing sequence, and assigned time of the CAV platoons. In particular, the solution ω is represented by a set of platoon vectors with a length l, which is determined by the sum of the number of platoon vectors l_z from different directions at the intersection. Each platoon vector in the solution contains the key information, e.g., formation pattern, passing sequence, and assigned time of a CAV platoon. These platoon vectors are placed based on the passing sequence of the CAV platoons. An example solution in the proposed hybrid ABC algorithm is illustrated in Fig. 3. Note that the length of the vector set (total number of platoon vectors) in the solution can be revised in the proposed algorithm. The stored information in the platoon vectors is then updated based on the new set of platoon vectors through a random generation process, which will be shown in the solution initialization and renewal subsection in detail.

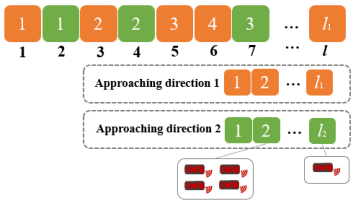

Fig. 3. Solution representation with a vector of length l including two directions

C. Solution initialization and renewal

An empty solution ω is established to store the decision information of the CAV platoons. The number of the platoon vectors in each direction is randomly generated under the total number of CAVs constraint. The vector set consisting of the platoon vectors can be first built in the solution and the length of the vector set is the sum of the generated number of platoon vectors in all directions. The CAVs from the vehicle set can be randomly assigned to the platoon vectors in the same direction if the assignment does not violate the no-overtaking rule and the restrictions of the upper bound of platoon size and the total number of CAVs in each direction. Moreover, the passing sequence of the CAV platoons is randomly determined and used for placing the platoon vectors in the solution. Based on the generated passing sequence, the assigned time of the first CAV platoon is randomly generated under the constraint of the minimum travel time of the first CAV in the platoon. Furthermore, the assigned times of the remaining CAV platoons are determined based on the assigned time of the first CAV platoon, the number of CAVs in these platoons obtained by formation pattern, and the generated passing sequence. As a result, a solution is created while the key information, e.g., platoon patterns, passing sequence, and assigned time of the CAV platoons, are stored in these platoon vectors. Following the requirements of the ABC algorithm, there are N solutions needed to be initialized, whose number equals that of employed bees and onlooker bees. The above procedure is repeated to generate all the solutions.

The core idea of solution renewal is to update the decision information based on the new number of platoon vectors generated by the neighborhood operator. For the formation pattern, the CAV platoons can be randomly formed by CAVs under the constraints of the total number of CAVs and the upper bound of platoon size in each direction. The passing sequence of the CAV platoons satisfying no-overtaking rules in the same directions is randomly determined. The assigned time of the CAV platoon with the first right of way is also updated using the neighborhood operator. Based on the above decision information, the assigned times of the remaining CAV platoons are generated. Afterward, the total travel delays of all the CAVs and total errors of the terminal performance measures of the CAV platoons are calculated and the fitness value is then determined for each solution. The generated solution yielding better fitness value can be recorded and viewed as a new solution, and the old solution will be abandoned.

D. Neighborhood operator

In the proposed hybrid ABC algorithm, a neighborhood operator is adopted for the employed bees and onlooker bees to generate the decision variables Φ of the new solution near the current solution. In the employed bee phase during each iteration of the algorithm, the decision variables of the new solution are generated based on Eq. (24) by combining the decision variables in the current solution and the neighborhood solution randomly selected by the operator. In our study, the number of platoon vectors in each direction and the assigned time of the first CAV platoon in the solution can be updated in each iteration. If the fitness value of the new solution is better than that of the current solution, the old one is replaced by the new one and the limit of the solution is 0. Otherwise, the old solution keeps unchanged and the count of the limit is increased by 1. In the onlooker bee phase, the operator first randomly chooses a solution using the roulette wheel method (introduced in section 4.2.5) for a neighborhood search.

Similarly, the new solution will replace the old one if the new solution has a better fitness value than the old one. The count of the limit is set as 0 or increased by 1 if the current solution is replaced or not replaced, respectively. The decision variables in the new solution can be generated by

$$\Phi_i^{new} = \Phi_i^{old} + \varphi \times (\Phi_i^{old} - \Phi_m^{neigh}), \forall \Phi \in \{l_z, t_z^1\}, m \in \{1,2,...,N\} \setminus \{i\} \quad (24)$$

where φ is a random number within the range [-1, 1].

E. Selection of solution sources

Let $T(\omega_i)$ be the total travel delays of all the CAVs for the solution ω_i. Let $E(\omega_i)$ be the total errors between the output and pre-specified terminal performance measures of the CAV platoons for the solution ω_i. Therefore, the objective value of the solution ω_i can be calculated by

$$OBJ(\omega_i) = T(\omega_i) + \gamma E(\omega_i) \quad (25)$$

where γ is the weighing parameter of the total errors.

During each iteration of the algorithm, the onlooker bee uses the roulette wheel method to select the solution based on the shared information by the employed bee. The method is essentially a probabilistic selection scheme, the better the fitness value the solution *i* has, the higher the probability of the solution *i* can be selected. The detailed calculation of the roulette wheel method is shown as follows:

$$P_i = \frac{f(\omega_i)}{\sum_{m=1}^{N} f(\omega_m)} \quad (26)$$

with

$$f(\omega_i) = \begin{cases} 1/(1+OBJ(\omega_i)), & \textbf{if } OBJ(\omega_i) \geq 0 \\ 1+abs(OBJ(\omega_i)) & \textbf{if } OBJ(\omega_i) < 0 \end{cases} \quad (27)$$

where $f(\omega_i)$ is the fitness value of the solution *i* in the hybrid ABC algorithm.

V. Dynamic Programming Algorithm for Optimal Control Model for Platoon Formation

Unlike the existing works that focus on solving the following CAVs' trajectories in the platoon without considering the restrictions of terminal performance measures of the platoons [20], [28], our study is to obtain the feasible trajectories of CAVs to form the platoons while traversing the conflict point and reaching the pre-specified terminal headway and speed. That is, the first CAV, the following CAVs, and all the CAVs in the platoons need to reach the conflict point, the pre-specified headway, and the pre-specified speed, respectively. The realization of platoon formation requires precise controls of CAV trajectories during the assigned time horizon, which can be formulated as the constrained optimal control problem. Therefore, the optimal trajectories of CAVs for platoon formation can be obtained by minimizing the total cost composed of the running and terminal costs during the assigned time horizon. Considering the restrictions of platoon formation, the formulations of the running and terminal costs in the cost function need to be re-designed in our study. Details will be found in the ensuing.

A. Cost functions of the optimal control model for platoon formation of CAVs

To facilitate the precise arrival of the first CAV in the *k*th platoon of the direction *z* to the conflict point with the pre-specified terminal speed under the given assigned time t_z^{k*}, we formulate the terminal cost of the first CAV in the platoon, i.e., $\zeta\left(\boldsymbol{x}_z^k(t_z^{k*})\right)$. The terminal cost of the first CAV in the *k*th platoon of the direction *z* is calculated by

$$\zeta\left(\boldsymbol{x}_z^k(t_z^{k*})\right) = \frac{1}{2}\alpha_1\left[p_1(t_z^{k*}) - \hat{p}\right]^2 + \frac{1}{2}\alpha_2\left[v_1(t_z^{k*}) - \hat{v}\right]^2, \forall z \in \boldsymbol{Z}, k = 1,2,...,|\boldsymbol{I}_z| \quad (28)$$

where p_1 and v_1 is the position and speed of the first CAV in the *k*th platoon of indirection *z* at the time t_z^{k*}, respectively, and α_1 and α_2 are the weighting coefficients of position and speed errors of the first CAV in the platoon, respectively.

Since the running cost is associated with the cost of the transition process before the CAVs reach the steady car-following state, it needs to consider the system state and acceleration at each time step within the assigned time horizon. To realize the platoon formation where the following CAVs can maintain the pre-specified terminal headway and speed, the running cost should include three cost terms. The first term is formulated to regulate the actual headway toward the pre-specified terminal headway, the second term is to maintain the speed homogeneity between the two CAVs, and the last term is used to ensure comfortable and energy-efficient motion over the time horizon. The running cost of the *k*th platoon in the direction *z* at the time *t* is formulated as follows:

$$\begin{aligned} \mathcal{L}\left(\boldsymbol{x}_z^k(t), \boldsymbol{u}_z^k(t)\right) = \frac{1}{2}\sum_{i=2}^{n}\Bigg(& \beta_1\left(p_{i^+}(t) - p_i(t) - \hat{d}\right)^2 \\ & + \beta_2\left(v_{i^+}(t) - v_i(t)\right)^2 + \beta_3 u_i(t)^2\Bigg) \\ & + \frac{1}{2}\beta_3 u_1(t)^2, \forall t \in \left[t^0, t_z^{k*}\right) \end{aligned} \quad (29)$$

where $p_{i^+}(t) - p_i(t), \forall t \in \left[t^0, t_z^{k*}\right)$ is the actual headway between two consecutive CAVs in the *k*th platoon of the indirection *z* at the time *t* where $n = \left|\boldsymbol{I}_z^{k*}\right|$, $u_1(t)$ is the acceleration of the first CAV in the *k*th platoon of the indirection *z* at the time *t*, and β_1, β_2, and β_3 are the weighting parameters of the three cost terms.

B. Solving procedures of the model $\left[OC_z^k\right]$

For ease of obtaining the trajectories of CAVs for platoon formation, the continuous-time process of optimal control formulation can be approximated by a discrete-time process. As a result, the cost function in Eq. (1) in a discrete form can be written as follows:

$$J = \sum_{r=0}^{R-1}\mathcal{L}(\boldsymbol{x}_z^k(r), \boldsymbol{u}_z^k(r))\Delta t + \zeta(\boldsymbol{x}_z^k(R)), \forall z \in \boldsymbol{Z}, k = 1,2,...,|\boldsymbol{I}_z| \quad (30)$$

where Δt and *r* are the length and index of the control step, respectively, and *R* is the total control steps.

The system dynamics model in Eq. (2) following the linear law in a discrete form is presented as follows:

$$\boldsymbol{x}_z^k(r+1) = \boldsymbol{A}_r\boldsymbol{x}_z^k(r) + \boldsymbol{B}_r\boldsymbol{u}_z^k(r), \forall z \in \boldsymbol{Z}, k = 1,2,...,|\boldsymbol{I}_z|, r \in \{0,...,R-1\} \quad (31)$$

where $\boldsymbol{A}_r$ and $\boldsymbol{B}_r$ are system dynamic matrices in discrete form.

Here, we will introduce the dynamic programming algorithm with the new formulation of cost functions step by step to solve the model $\left[OC_z^k\right]$. The detailed steps are illustrated as follows:

Step 1: Discrete the time horizon $\left[t^0, t_z^{k*}\right]$ into R control steps and obtain the value of control step Δt, i.e., $\Delta t = (t_z^{k*} - t^0)/R$.

Step 2: Calculate the coefficient matrix of the system dynamics model in the discrete form, i.e., $\boldsymbol{A}_r$ and $\boldsymbol{B}_r$ as follows:

$$\mathbf{A}_r = \mathbf{I}_{n\times n} + \mathbf{A}\times\Delta t \tag{32}$$

$$\mathbf{B}_r = \mathbf{B}\times\Delta t \tag{33}$$

Step 3: Calculate the weighting matrices in the running cost function for $r\in\{0, 1, \ldots, R\}$, i.e., $\boldsymbol{Q}_r$, $\boldsymbol{D}_r$, and $\boldsymbol{O}_r$. Based on the new formulations of the terminal and running costs, we have:

$$\mathbf{Q}_r = \tilde{\mathbf{Q}}_r \times \Delta t \tag{34}$$

$$\mathbf{D}_r = 0 \tag{35}$$

$$\mathbf{O}_r = \tilde{\mathbf{O}}_r \times \Delta t \tag{36}$$

where $\tilde{\mathbf{Q}}_R = \begin{bmatrix} \tilde{\mathbf{Q}}_{R1}^{n\times n} & 0^{n\times n} \\ 0^{n\times n} & \tilde{\mathbf{Q}}_{R2}^{n\times n} \end{bmatrix}$, $\tilde{\mathbf{Q}}_{R1} = \begin{bmatrix} \alpha_1+\beta_1 & \beta_1 & & & \\ -\beta_1 & 2\beta_1 & \ddots & & \\ & \ddots & \ddots & \ddots & \\ & & \ddots & 2\beta_1 & \beta_1 \\ & & & -\beta_1 & \beta_1 \end{bmatrix}$,

$\tilde{\mathbf{Q}}_{R2} = \begin{bmatrix} \alpha_2+\beta_2 & \beta_2 & & & \\ -\beta_2 & 2\beta_2 & \ddots & & \\ & \ddots & \ddots & \ddots & \\ & & \ddots & 2\beta_2 & \beta_2 \\ & & & -\beta_2 & \beta_2 \end{bmatrix}$ for control step R,

$\tilde{\mathbf{Q}}_r = \begin{bmatrix} \tilde{\mathbf{Q}}_{r1}^{n\times n} & 0^{n\times n} \\ 0^{n\times n} & \tilde{\mathbf{Q}}_{r2}^{n\times n} \end{bmatrix}$, $\tilde{\mathbf{Q}}_{r1} = \begin{bmatrix} \beta_1 & \beta_1 & & & \\ -\beta_1 & 2\beta_1 & \ddots & & \\ & \ddots & \ddots & \ddots & \\ & & \ddots & 2\beta_1 & \beta_1 \\ & & & -\beta_1 & \beta_1 \end{bmatrix}$,

$\tilde{\mathbf{Q}}_{r2} = \begin{bmatrix} \beta_2 & \beta_2 & & & \\ -\beta_2 & 2\beta_2 & \ddots & & \\ & \ddots & \ddots & \ddots & \\ & & \ddots & 2\beta_2 & \beta_2 \\ & & & -\beta_2 & \beta_2 \end{bmatrix}$ for control step $r\in\{0, 1, \ldots, R\text{-}1\}$, and $\tilde{\mathbf{O}}_r^{n\times 1} = \begin{bmatrix} \beta_3 \\ \vdots \\ \beta_3 \end{bmatrix}$ for control step $r\in\{0, 1, \ldots, R\}$.

Step 4: At control step R, the optimal solutions of $\hat{\mathbf{Q}}_R$, $\hat{\mathbf{D}}_R$, and $\hat{\mathbf{E}}_R$ are:

$$\hat{\mathbf{Q}}_R = \mathbf{Q}_R \tag{37}$$

$$\hat{\mathbf{D}}_R = 0 \tag{38}$$

$$\hat{\mathbf{E}}_R = 0 \tag{39}$$

Step 5: Calculate concomitant matrices backward, i.e., $\hat{\mathbf{Q}}_r$, $\hat{\mathbf{D}}_r$, and $\hat{\mathbf{E}}_r$, for $r\in\{R\text{-}1, \ldots, 1, 0\}$ based on the matrices of control step R:

$$\hat{\mathbf{Q}}_r = \mathbf{G}_r^T\mathbf{O}_r\mathbf{G}_r + \mathbf{S}_r^T\hat{\mathbf{Q}}_{r+1}\mathbf{S}_r + \mathbf{Q}_r \tag{40}$$

$$\hat{\mathbf{D}}_r = \mathbf{G}_r^T\mathbf{O}_r\mathbf{H}_r + \mathbf{S}_r^T\hat{\mathbf{Q}}_{r+1}\mathbf{T}_r + \mathbf{S}_r^T\hat{\mathbf{D}}_{r+1} + \mathbf{D}_r \tag{41}$$

$$\hat{\mathbf{E}}_r = \frac{1}{2}\mathbf{H}_r^T\mathbf{O}_r\mathbf{H}_r + \frac{1}{2}\mathbf{T}_r^T\hat{\mathbf{Q}}_{r+1}\mathbf{T}_r + \mathbf{T}_r^T\mathbf{D}_{r+1} + \hat{\mathbf{E}}_{r+1} + \mathbf{E}_r \tag{42}$$

with

$$\mathbf{P}_r = (\mathbf{O}_r + \mathbf{B}_r^T\hat{\mathbf{Q}}_{r+1}\mathbf{B}_r)^{-1} \tag{43}$$

$$\mathbf{G}_r = -\mathbf{P}_r\mathbf{B}_r^T\hat{\mathbf{Q}}_{r+1}\mathbf{A}_r \tag{44}$$

$$\mathbf{H}_r = -\mathbf{P}_r\mathbf{B}_r^T(\hat{\mathbf{Q}}_{r+1}\mathbf{C}_r + \hat{\mathbf{D}}_{r+1}) \tag{45}$$

$$\mathbf{S}_r = \mathbf{A}_r + \mathbf{B}_r\mathbf{G}_r \tag{46}$$

$$\mathbf{T}_r = \mathbf{B}_r\mathbf{H}_r + \mathbf{C}_r \tag{47}$$

Step 6: Calculate the system state and acceleration vector of the CAV platoons forward for $r\in\{0, 1, \ldots, R\text{-}1\}$:

$$\mathbf{u}(r) = \min\left[\max(\mathbf{G}_r\mathbf{x}(r) + \mathbf{H}_r, a_{\min}), a_{\max}\right] \tag{48}$$

$$\mathbf{x}(r+1) = \mathbf{S}_r\mathbf{x}(r) + \mathbf{T}_r \tag{49}$$

C. Constraints

Moreover, since the solved system state in Eq. (49) cannot ensure the speed within the bound and collision-free between the consecutive CAVs in the same or different platoons, the system state and acceleration need to add constraints during the solving process of the algorithm. In this respect, the algorithm can re-calculate the trajectories of CAVs for platoon formations according to the bounds of the acceleration, speed, and safety distance as long as the solved trajectories at any control step violate the acceleration, speed, or collision constraints. The trajectory adjustments will be made with the following steps:

(i) During the execution process of the algorithm at each control step, the acceleration of the CAVs in the platoons can be first obtained based on the initial motion state and given input information.

(ii) Check whether the solved acceleration satisfies the acceleration constraints. If it is satisfied, then go to step 3; If not, the acceleration at the control step is set to be the upper or lower bound of acceleration.

(iii) Check whether the speed calculated by the kinetic equation satisfies the speed constraints. If it is satisfied, then go to step 4; If not, the speed at the control step is set to be the upper or lower bound of speed, and the acceleration can then be re-calculated according to the speed constraint.

(iv) Check the position calculated by the kinetic equation whether it ensures collision avoidance with the immediate predecessor. If it is satisfied, the acceleration, speed, and position at the control step satisfying the acceleration, speed,

and collision-free constraints are determined; If not, the position at the control step is set to be the difference between the position of the predecessor and safety distance. The speed and acceleration at the control step can be further re-calculated according to the position, speed, and acceleration constraints, so that their values are ensured within the feasible range.

(v) After the iterations of all control steps, the optimal acceleration, speed, and position trajectory during the assigned time horizon satisfying the acceleration, speed, and safety constraints can be ultimately obtained for all CAVs in the platoons.

VI. NUMERICAL EXPERIMENTS

In this section, we first conduct numerical experiments to validate the computation accuracy and solution quality of the proposed model and solution algorithm in contrast to the enumeration method. Second, numerical experiments are conducted to investigate the impacts of balanced and unbalanced motion states between approaching directions on the MPS. Third, the comparison experiments are carried out to demonstrate the effectiveness of the proposed platoon-based control strategy in terms of total travel delay and throughput against the benchmark strategy.

In the proposed hybrid ABC algorithm, there are three parameters needed to be set, i.e., the maximum number of iterations, the number of food sources, and the value of the limit. Considering the trade-off between computation time and solution quality in the preliminary experiments, the bee colony size is set to be 80 in which the number of employed bees and onlooker bees is identical and each one is 40. The maximum number of iterations is set as 300 and the value of the limit is fixed to 80 unless specified otherwise.

For the parameter setting in the numerical experiments, the maximum speed for the CAVs traversing the conflict point is set to be 16m/s according to the previous studies [1], [38]. Considering the application of the vehicle automation system, the desired spacing distance of passing the conflict point for the CAVs running in the platooning mode is 12m (the product of the time gap of 0.75s) and the desired spacing is 16m by gathering the spacing and the safety buffer distance of 4m [9], [39]. The desired spacing distance of passing the conflict point kept by the CAVs running individually in the same and different approaching directions is 25.6m and 28.8m (the corresponding time gap of 1.35s and 1.55s, respectively). The initial speed and headway of the CAVs in the vicinity of the intersection follow the uniform distributions in each direction, i.e., $v(t^0) \sim v_0 - \lambda_v U(0,1)$ and $s(t^0) \sim s_0 - \lambda_s U(0,1)$, where v_0, s_0, λ_v, and λ_s are larger than 0, and $U(0, 1)$ is the standard uniform distribution [1]. For simplicity, the distance between the decision location and the conflict point is fixed to be 160m for each direction within the intersection, which is referential to the existing studies [15], [33]. All the test instances are run for 20 times. As indicated by the previous studies (Bai et al., 2019; Zhang et al., 2020), the sufficient conditions ensuring string stability of CAV platoons are closely related to the parameters in the cost functions of optimal control models of CAVs, i.e., β_1, β_2, and β_3, which are coefficients representing the relative preference to headway error, speed difference, and acceleration. Specifically, the CAV platoons can ensure string stability only when the coefficients in the cost function of the optimal control model are larger than 0. Therefore, the parameter setting in our study can be set based on the stability conditions. The other parameter settings for the numerical experiments are elaborated in Table II.

Table II Parameter settings for numerical experiments

Parameter	Notation	Value
Time step	Δt	0.1 s
Safety distance	L	4 m
Minimum acceleration	$a_{\min}$	3 m/s^2
Maximum acceleration	$a_{\max}$	-5 m/s^2
Minimum speed	$v_{\min}$	0 m/s
Maximum speed	$v_{\max}$	16m/s
Weighing parameters of the following CAVs	β_1, β_2, β_3	10^3, 10^3, 1
Weighing parameters of the leading CAV	α_1, α_2	10^5, 10^3
Weighing parameter in the objective function	γ	10^2

A. *Performance comparisons of different algorithms*

To assess the performance of the proposed hybrid ABC algorithm, we compare the results of the proposed solution algorithm with the ones obtained by solving the proposed model using the enumeration method and the hybrid ABC algorithm with the first-in-first-out (FIFO) rule. The total number of CAVs can largely affect the model size and accordingly the computational efficiency of the solution algorithm. Therefore, we consider three crossing cases between two approaching directions at the intersection with the different total numbers of CAVs, i.e., 8, 10, and 12, in the two directions (4, 5, and 6 CAVs in each direction). The input parameters for these experiments are shown below: s_0 = 25 m, v_0 =15 m/s, λ_v = 1, and λ_s = 1. For the application of the enumeration method, a recursive function is coded to generate all possible solutions for each of these cases. We further develop a hybrid ABC algorithm using the FIFO rule to determine the passing orders of CAV platoons, which is referred to as the hybrid ABC algorithm (FIFO). Moreover, both the proposed hybrid ABC algorithm, hybrid ABC algorithm (FIFO), genetic algorithm, and enumeration method are implemented to solve the model for each of these cases under a limit of 0.5h.

The performance comparison results of the different methods under the three cases are shown in Table III. For the three methods, we show the optimal objective function values, the MPS values in two directions, and the computation time to obtain the solutions. The enumeration method is applied as a baseline method to obtain the global optimal solutions for checking the solution quality achieved by the proposed hybrid ABC algorithm. In addition to the enumeration method, in the revised manuscript, we have added the comparison analysis of the proposed hybrid ABC algorithm with FIFO and the traditional optimization algorithms of GA. The detailed results are presented in Table III. It indicates that the proposed hybrid ABC algorithm, hybrid ABC algorithm (FIFO), and genetic algorithm can find the solutions for all three cases within 0.5 h on average. On the contrary, the enumeration method only determines the solutions for the first two small-scale cases with a total number of 8 and 10 CAVs (4 and 6 CAVs for each direction) under the limit of computation time. It cannot give us a feasible solution after checking all possible solutions within the pre-specified computation time, when the total

number of CAVs increases to 12 (6 CAVs for each direction). We also report the computation time required to find the optimal solution by the enumeration method, which is 2.57 h. Furthermore, it can be seen that the proposed hybrid ABC algorithm can find the same global optimal solutions with less computation time obtained by the enumeration method. The proposed algorithm also obtained better solutions than the other benchmark algorithms, i.e., hybrid ABC algorithm (FIFO) and genetic algorithm, with comparable computation time, due to the hybrid ABC algorithm (FIFO) and genetic algorithm having larger objective values and not finding the optimal MPS values under the three cases. The MPS values obtained can deviate from the optimal ones as the number of CAVs increases. In conclusion, the experimental results demonstrate the superiority of the proposed solution algorithm in the computational efficiency and solution quality of the proposed model.

Table III Performance comparisons between different methods under three cases

Case	Method	Objective value	MPS1	MPS2	Computation time
8 CAVs	Enumeration	25.22	3.5	2.5	34.9 s
	Hybrid ABC (FIFO)	27.09	3.6	2.3	86.8 s
	Genetic algorithm	25.34	3.3	2.7	88.0 s
	Hybrid ABC	25.22	3.5	2.5	90.3 s
10 CAVs	Enumeration	36.09	3.4	3.6	374.5 s
	Hybrid ABC (FIFO)	37.81	3.3	3.6	292.7 s
	Genetic algorithm	37.25	3.2	3.4	284.1 s
	Hybrid ABC	36.09	3.4	3.6	300.1 s
12 CAVs	Enumeration	47.80	4.1	4.1	2.57 h
	Hybrid ABC (FIFO)	49.30	4.6	3.6	0.17 h
	Genetic algorithm	48.13	4.3	3.9	0.17 h
	Hybrid ABC	47.80	4.1	4.1	0.18 h

B. Analysis of maximum platoon size under different motion state scenarios

In this subsection, we investigate the impacts of balanced and unbalanced motion states on the MPS for crossing cases between two directions. The tested scenarios are constituted by two types of initial spacing headway (i.e., 25 m and 40 m) and initial speed (i.e., 10 m/s and 15 m/s) of CAVs in the two directions and a total number of 20 CAVs (10 CAVs for each direction) is considered. The input data for the experiments is $\lambda_v = 1$ and $\lambda_s = 1$ for all the scenarios, which is the same in the rest of the study unless stated. The MPS results under the balanced and unbalanced scenarios are elaborated in Table IV. Moreover, Fig. 4 shows the MPS results under all the scenarios. As for the balanced scenarios, i.e., S1, S2, S3, and S4, where the CAVs in the two directions have balanced headway and speed, there are similar MPS results for the two directions under the four scenarios as illustrated in Fig. 4(a). This is attributed to the fact by the homogeneities in headway and speed of CAVs between the two directions. The MPS under scenario S1 is similar to one under scenario S2 for the 25m headway setting, and similar MPS results can be also found under scenarios S3 and S4 for the headway of 40m. It implies that the initial speed of 15m/s and 10m/s has no significant effects on the MPS. On the contrary, we can see from Fig. 4(a) that the MPS under scenarios S1 and S2 are larger than that under scenarios S3 and S4. It is noticed that the headway can mainly contribute to the differences in MPS, and an initial large headway is not favorable to constitute a large-size platoon. The reason is that the large headway is relatively difficult to cluster the CAVs into a tight platoon, which leads to the formation of a small-size platoon.

Table IV MPS results under balanced and unbalanced motion state scenarios

Type	Scenario	Headway1	Headway2	Speed1	Speed2	MPS1	MPS2
Balanced	S1	25m	25m	15m/s	15m/s	5.2	5.3
	S2	25m	25m	10m/s	10m/s	4.9	4.8
	S3	40m	40m	15m/s	15m/s	1.8	2.0
	S4	40m	40m	10m/s	10m/s	1.8	2.0
Unbalanced	S5	25m	25m	15m/s	10m/s	3.4	4.6
	S6	40m	40m	15m/s	10m/s	1.6	1.8
	S7	25m	40m	15m/s	15m/s	3.9	2.0
	S8	25m	40m	10m/s	10m/s	4.3	1.9

The MPS results under the unbalanced scenarios, i.e., S5, S6, S7, and S8, are illustrated in Fig. 4(b). It can be seen that the MPS in direction 1 with the speed of 15m/s is smaller than that in direction 2 with the speed of 10m/s under scenario S5 for the same headway of 25m. The reason is that the CAVs in the high-speed direction 1 can easily catch up with predecessors for achieving platoon formation and prefer to pass the intersection as soon as possible. Nevertheless, a too large-size platoon in indirection 1 is not favorable to the passing of CAVs in the low-speed direction 2. Therefore, the multiple small-size platoons in the high-speed direction are formed with the aid of high speed and small headway. On the contrary, the CAVs in direction 2 are prone to form a platoon for efficiency improvements to overcome the negative impacts of the low speed. As a result, a large MPS in the low-speed direction can be generated. Moreover, different MPS results can be observed under scenario S6 with the unbalanced speed and balanced headway of 40m between the two directions. In particular, there is a similar MPS result between the two directions, and both are smaller than 2. It suggests that the large headway is not beneficial to cluster the CAVs into a large-size platoon in any direction. Under scenarios S7 and S8 with the unbalanced headway and balanced speed between the two directions, the MPS are close to 4 and 2 in the small and large headway directions, respectively. It indicates that the CAVs in direction 1 can fully utilize the small headway to group more CAVs into a platoon regardless of the speeds.

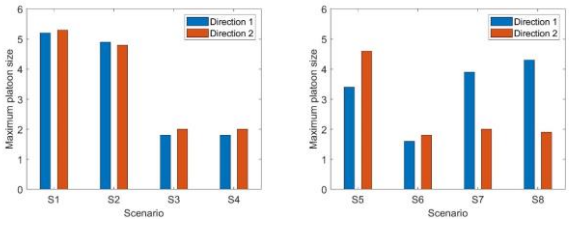

(a) (b)

Fig. 4. MPS results: (a) balanced scenarios; (b) unbalanced scenarios

Moreover, we examine the differences in MPS between balanced and unbalanced state scenarios as illustrated in Fig. 5. Based on the comparisons of the MPS between unbalanced scenario S5 and balanced scenarios S1 and S2, we can find that the MPS value in low-speed direction 2 maintains close to that under scenarios S1 and S2, and the MPS in high-speed direction 1 is reduced than that under scenarios S1 and S2 in Fig. 5(a). As mentioned above, the reductions in MPS in high-speed direction are beneficial to mitigate the unbalanced speed between the two directions for overall efficiency improvement. The MPS values under scenario S6 with balanced headway and unbalanced speed are is slightly smaller than that under

scenarios S3 and S4 in Fig. 5(b). The above results indicate that the speed imbalance between the two directions can diminish the platoon formation and thus result in a reduced MPS. As for scenario S7 with the unbalanced headway and balanced speed, the MPS is 3.9 in the small-headway direction 1, which is smaller and larger than that under scenarios S1 and S3, respectively, and a pretty small MPS of 2.0 in the large-headway direction 2 is kept similar to that under scenario S3 in Fig. 5(c). The similar comparison results of MPS between scenario S8 and scenarios S2 and S4 can be found in Fig. 5(d). This implies that the increments and reductions in headway can be beneficial to diminish and facilitate the formation of a large-size platoon, respectively.

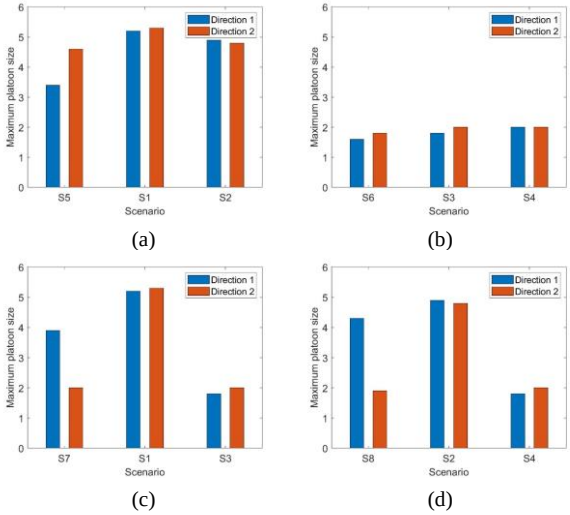

(a) (b) (c) (d)

Fig. 5. MPS comparison results between balanced and unbalanced scenarios

C. Performance analysis of the platoon-based cooperative control

This subsection presents the traffic performance of the proposed platoon-based cooperative signal-free control strategy under the restriction of obtained MPS in multiple performance aspects. Numerical experiments are conducted for crossing cases of 20 CAVs between two directions (10 CAVs for each direction) under balanced and unbalanced motion state scenarios. Three measurements of effectiveness, i.e., total travel delay and throughput, are adopted to present the traffic performance. The throughput is calculated based on the total number of CAVs divided by the difference between the travel time of the last CAV passing the conflict point and the initial time instant.

1) Balanced motion state scenarios

The influence of the headway and speed in the two directions on the traffic performance at intersections are investigated for the platoon-based and vehicle-based control strategies. The performance results for the two control strategies under balanced scenarios are presented in Table V. It can be seen that the proposed platoon-based strategy can improve the throughput by 12% under balanced scenarios compared with the benchmark method. It suggests the effectiveness of the platoon-based strategy in improving traffic performance. The reason is that the CAVs can group into platoons to pass the intersections under most scenarios, which leads to improvements in traffic performance. Moreover, it can be seen that the results of the total travel delay and throughput become worse as the speed decreases from 15m/s under scenario S1 to 10m/s under scenario S2 for the proposed strategy. Similarly, the performance under scenario S4 is not as good as that under scenario S3 as the speed reduces. This is because the CAVs at a high speed can adjust their motion state to reach the pre-specified terminal state as soon as possible. Moreover, although the throughput performance are not improved under scenario S3 compared with scenario S1,

Table V Performance comparison of vehicle-based and platoon-based strategies under balanced scenarios

Method	Scenario	Headway1	Headway2	Speed1	Speed2	Delay(s)	Error	Throughput (veh/h)
Vehicle-based	S1	25m	25m	15m/s	15m/s	191.07	0.039	1701
	S2	25m	25m	10m/s	10m/s	213.76	0.031	1658
	S3	40m	40m	15m/s	15m/s	117.72	0.028	1672
	S4	40m	40m	10m/s	10m/s	139.02	0.029	1630
Platoon-based	S1	25m	25m	15m/s	15m/s	150.06	0.049	1933
	S2	25m	25m	10m/s	10m/s	161.92	0.097	1890
	S3	40m	40m	15m/s	15m/s	118.40	0.028	1655
	S4	40m	40m	10m/s	10m/s	140.06	0.017	1623

Table VI Performance comparison of vehicle-based and platoon-based strategies under unbalanced scenarios

Method	Scenario	Headway1	Headway2	Speed1	Speed2	Delay(s)	Error	Throughput (veh/h)
Vehicle-based	S5	25m	25m	15m/s	10m/s	195.72	0.033	1697
	S6	40m	40m	15m/s	10m/s	121.50	0.024	1670
	S7	25m	40m	15m/s	15m/s	152.23	0.034	1698
	S8	25m	40m	10m/s	10m/s	174.38	0.026	1647
Platoon-based	S5	25m	25m	15m/s	10m/s	145.80	0.040	1927
	S6	40m	40m	15m/s	10m/s	122.33	0.021	1659
	S7	25m	40m	15m/s	15m/s	121.83	0.029	1794
	S8	25m	40m	10m/s	10m/s	149.80	0.023	1734

the total travel delay can be reduced when the headway increases from 25m under scenario S1 to 40m under scenario S3. It indicates that more CAVs with a small headway are easier to form a platoon, which is beneficial to improving the traffic performance in throughput. However, lots of travel time needs to be spent on frequent motion adjustments for platoon formation, which results in an increment in total travel delay. We can observe that there are similar comparison results in

total travel delay and throughput between scenarios S2 and S4. In addition, it is also noticed that the total errors of terminal performance measures are smaller than 0.05 under all the balanced scenarios. The results indicate that the optimal trajectories of CAVs for platoon formation are feasible for practical application with the platoon-based control strategy.

Fig. 6 illustrates the example CAV trajectories for the platoon-based control strategy under the balanced scenarios. With the platoon-based control strategy, the CAVs can form the platoons to transverse the conflict point under balanced scenarios with small headway as illustrated in Figs. 6(a) and 6(b). It can be seen that the CAVs between the two directions can pass the conflict point individually and alternately under the balanced scenarios with large headway in Figs. 6(c) and 6(d), and the CAVs in the same direction pass the conflict point more diversely under the large headway and small speed setting in Fig. 6(d). Moreover, we can observe that the smooth CAV trajectories are obtained based on the optimal control scheme for the proposed strategy.

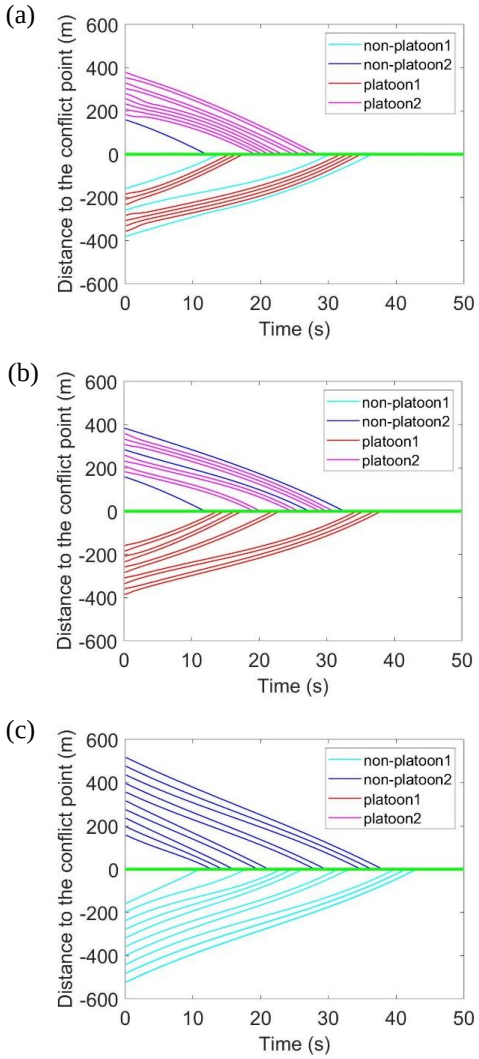

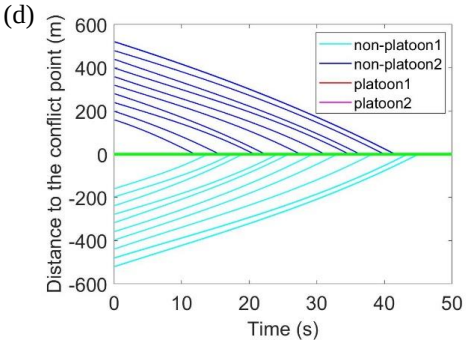

Fig. 6. Illustration of CAV trajectories between two directions under the balanced scenarios: Figs. 6(a), (b), (c), and (d) for scenarios S1, S2, S3, and S4, respectively

2) Unbalanced motion state scenarios

The performances of vehicle-based and platoon-based control strategies under unbalanced scenarios are presented in Table VI. We can see that the proposed platoon-based strategy can improve the throughput by 4% to 11% under unbalanced scenarios compared with the benchmark method. It can be seen that the throughput values under scenario S5 are better than those under scenario S6 for the platoon-based strategy. The throughput performance can be also improved under scenario S7 compared with scenario S8. The improvements in throughput are attributed to the small headway or large speed setting that can facilitate the platoon formations. However, there exists a larger total travel delay under scenarios S5 and S8 than under scenarios S6 and S7, respectively. This is because the CAV whose initial motion states are closer to the pre-specified terminal states require more adjustments to accommodate the complex formation of CAV platoons under scenario S5. Under scenario S6, the CAVs are prone to drive individually and do not need to slow down frequently to form a platoon, leading to a small total travel delay. Moreover, the total travel delay is increased under scenario S8 compared with scenario S7 due to the small initial speeds.

Fig. 7 illustrates the example CAV trajectories for the platoon-based control strategy under unbalanced scenarios. Similarly, the CAVs in each direction can form the platoons to transverse the conflict point under the unbalanced scenarios with the small headway setting in the approaching direction as illustrated in Figs. 7(a), 7(c), and 7(d). The CAVs in the large headway direction can pass the conflict point separately. On the contrary, as shown in Figs. 7(a), (b), (c), and (d), the smooth trajectories of the CAV platoons obtained by the proposed platoon-based control strategy can be also presented under the unbalanced scenarios.

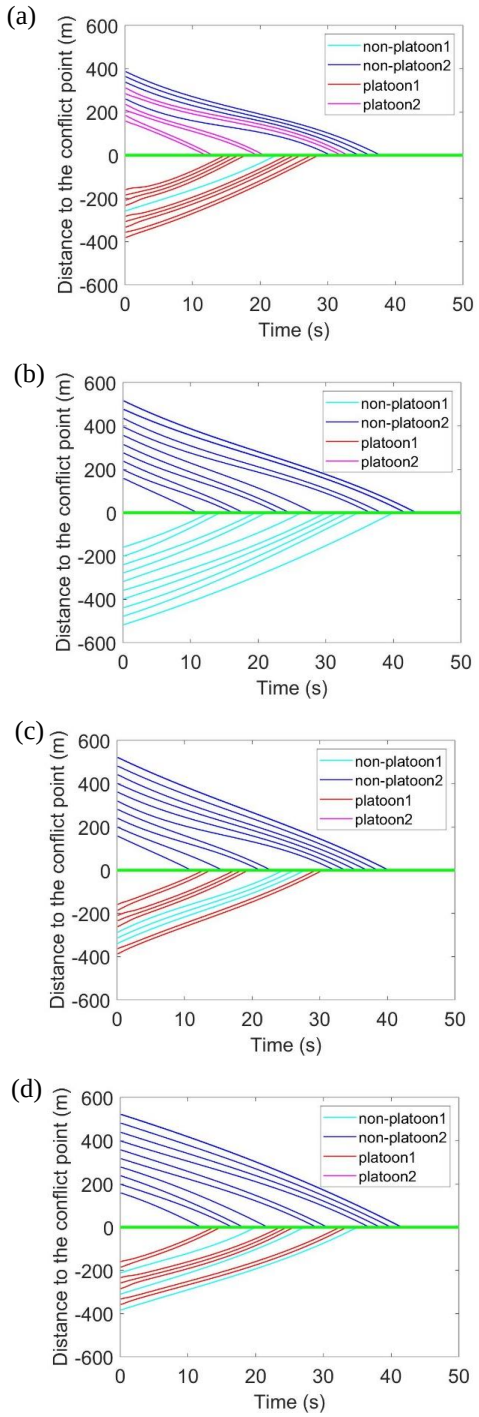

Fig. 7. Illustration of CAV trajectories between two directions under the unbalanced scenarios: Figs. 7(a), (b), (c), and (d) for scenarios S5, S6, S7, and S8, respectively

VII. Summary and Discussion

Based on the experimental results, we can see that the MPS can reach 5.0 at most in one direction among all scenarios. The MPS of the two directions are similar under balanced motion state scenarios and reduce under unbalanced speed scenarios than balanced motion state scenarios. Moreover, the MPS of the two directions can increase or reduce under unbalanced headway scenarios than balanced motion state scenarios, depending on the headway and speed combination between the two directions. In addition, the comparison results between the platoon-based and vehicle-based control strategies indicate that the platoon-based control strategy can improve the throughput by 12% under balanced scenarios and by 4% to 11% under unbalanced scenarios, which demonstrates the merits in improving traffic efficiency of the platoon-based control strategy. For the platoon-based control strategy, the small initial headways can be beneficial to improving the throughputs while increasing the total travel delays. The small initial speeds are not beneficial to improving the throughputs and total travel delays.

In this section, we would also like to present the potential of the proposed platoon-based control strategy for signal-free intersection management, in addition to determining the tactical platoon size threshold for signal-free intersection management while considering the influences of operational decisions. For the feasibility of the straightforward application, the management policy of maximum platoon size can be developed based on the obtained results of the platoon size thresholds, which provides a useful decision basis to transport authorities and automotive operators for signal-free intersection management. Moreover, based on the obtained size threshold results, we can restrict the search range of the platoon size for other models in real-time applications. Infeasible solutions that violate the maximum platoon size constraint can be excluded at the early stage, which can improve computational efficiency.

Moreover, for the real-time application of the proposed approach, we can transform the proposed optimization model (essentially a bi-level model) into a simplified optimization model by the rule applications, as suggested by previous studies [16], [20], [30]. For example, we can determine the formation patterns with a rule-based method considering the obtained size threshold results. That is, the CAVs are clustered into the same platoon if the headways are smaller than a grouping threshold under the restriction of the obtained maximum platoon size. The first-in-first-out (FIFO)/optimization algorithm has been extensively used to determine the passing sequences of CAV platoons. In this way, the computational efficiency will be significantly improved for model solving and the solutions can be found within a few seconds, which is feasible for the real-time application of the proposed platoon-based signal-free control approach. Nevertheless, the specified design for the real-time application of the proposed approach is not the focus of this study.

VIII. Conclusion and Future Works

In this study, we investigate the MPS for the PCSIC problem taking into account the platoon formation process of the CAVs in the vicinity of intersections. To this end, a novel mixed-integer nonlinear programming (MINLP) model is formulated by explicitly incorporating the platoon size limit and the CAV trajectories for platoon formation constraints. It can determine the optimal MPS, formation pattern, passing sequence, assigned time of the CAV platoons, and the trajectories of the CAVs to form the platoons by minimizing the total travel delays of all the CAVs. Due to the complicated structure of the proposed model, we propose a hybrid ABC algorithm integrating the ABC approach and dynamic programming

algorithm for an optimal control scheme to obtain good-quality solutions to the underlying problem. Numerical experiments are first conducted to validate the efficacy of the proposed model and solution algorithm. The impacts of balanced and unbalanced headway and speed on MPS are then investigated. At last, we make a performance analysis of the proposed platoon-based control strategy under balanced and unbalanced scenarios in aspects of travel delay and throughput.

Further research can be undertaken in the following several aspects. First, efficient solution algorithms remain to be developed to improve the solving efficiency for future implementation. Second, in the current study, the MPS configurations between two directions are investigated. The investigations of the MPS configurations in multiple directions at intersections will be considered. Moreover, the current study focuses on platoon formation for the CAVs and does not consider the scenarios where the CAV platoons already formed in the vicinity of the intersections, which probably results in the CAV platoon splitting. Thus, incorporating platoon splitting into the platoon-based cooperative signal-free intersection control is also worth to be studied. It is noticed that the proposed holistic framework also adapts to address the platoon splitting problems. Finally, it would be practically significant to extend the current works to achieve platoon-based cooperative control at intersections under mixed traffic flow conditions and consider pedestrians and non-motorized vehicles into intersection management of mixed traffic flow including multiple traffic participants. In future research, we will try to conduct validations by the experiments to further demonstrate the effectiveness of the model and solution algorithms.

IX. ACKNOWLEDGEMENT

The work of Yuan Zheng was supported by the Natural Science Foundation of Jiangsu Province (No. BK20241326), the start-up research fund of Southeast University (No. RF1028623243), and the State Key Laboratory of Intelligent Green Vehicle and Mobility under Project No. KFY2420. The work of Min Xu was supported in part by the Research Grants Council of the Hong Kong Special Administrative Region, China, under Project PolyU 15210620 and in part by The Hong Kong Polytechnic University under Grant 1-ZVPT. The work of Shining Wu was supported in part by the Hong Kong Research Grants Council under Grant 15508021. The work of Shuaian Wang was supported by the National Natural Science Foundation of China under Grant 72361137006.

APPENDIX

Table A. Notation list

Sets and Indices	
$\boldsymbol{Z}$	Set of approaching direction at the intersection
$\boldsymbol{I}_z^k$	Set of CAVs in the kth platoon formed of direction z
$\boldsymbol{\Psi}$	Output set of the model $\left[OC_z^k\right]$
$\tilde{\boldsymbol{\Psi}}$	Return set of the model $\left[OC_z^k\right]$
z, z'	Index for approaching direction
i, i^-	Index for CAVs
k, k'	Index for the order of CAV platoons
t	Index for time instant
r	Index for control step
$\boldsymbol{x}_z^k$	State column vector of the kth platoon in direction z
$\boldsymbol{u}_z^k$	Acceleration column vector of the kth platoon in direction z
$p_i(t)$	Position of CAV i at time t
$v_i(t)$	Speed of CAV i at time t
$u_i(t)$	Control input (i.e., acceleration prescribed by the controller) of CAV i at time t
J	Total cost for the optimal control scheme
$\mathcal{L}$	Running cost for the optimal control scheme
ζ	Terminal cost for the optimal control scheme
T	Total travel delays of all the CAVs
E	Total errors between the output and pre-specified terminal performance measures of the CAV platoons
t^0	Time instant when the most leading vehicle in the zone (e.g., CAV_1 in Fig. 1(a)) reaches the decision location of its direction
$\bar{t}_i$	Minimum travel time of vehicle i in direction z to reach the conflict point
$\tilde{p}_z^k$	Terminal position of a platoon represented by the terminal position of the first CAV in the platoon
$\tilde{d}_z^k$	Terminal headway of a platoon obtained by averaging the terminal headways of the following CAVs in the platoon
$\tilde{v}_z^k$	Terminal speed of a platoon by averaging the average terminal speeds of the CAVs in the platoon
$\tilde{\boldsymbol{t}}_z^k$	CAV additional time column vector of the kth platoon of the direction z to travel the additional distance (see the orange line in Fig. 1(b)) at the assigned time t_z^k with a constant speed
Parameters	
a_{min}	Minimum acceleration
a_{max}	Maximum acceleration
v_{min}	Minimum speed
v_{max}	Maximum speed
L	Safety buffer distance
$\beta_1, \beta_2, \beta_3$	Weighing parameters of the CAVs
α_1, α_2	Weighing parameters of the leading CAV
γ	Penalty weighing parameters
M	Large positive constant
$\hat{p}$	Intersection conflict point of approaching directions
$\hat{d}$	Pre-specified terminal headway
$\hat{v}$	Pre-specified terminal speed
Δt	Time step
D_c	Length of control zone
Decision Variables	
w_{zi}^k	Binary variables: 1, if vehicle i joins the kth platoon in the direction z; 0, otherwise
y_z^k	Binary variables: 1, if the kth platoon in direction z is a not null CAV platoon; 0, otherwise
c_z	Maximum allowable vehicle number in a CAV platoon of the direction z
$s_{kk'}$	Binary variables: 1, if the kth platoon in the direction z has the right of priority over the k' th platoon in the direction z'; 0, otherwise
t_z^k	Assigned time of the kth platoon in the direction z reaching the conflict point
$\boldsymbol{x}_z^k$	State trajectory vector of the kth platoon in direction z
$\boldsymbol{u}_z^k$	Acceleration vector of the kth platoon in direction z

REFERENCES

[1] X. Han, R. Ma, and H. M. Zhang, "Energy-aware trajectory optimization of CAV platoons through a signalized intersection," *Transp. Res. Part C Emerg. Technol.*, vol. 118, p. 102652, Sep. 2020, doi: 10.1016/j.trc.2020.102652.

[2] M. S. Rahman, M. Abdel-Aty, J. Lee, and M. H. Rahman, "Safety benefits of arterials' crash risk under connected and automated vehicles," *Transp. Res. Part C Emerg. Technol.*, vol. 100, pp. 354–371, Mar. 2019, doi: 10.1016/j.trc.2019.01.029.

[3] Y. Zheng, B. Ran, X. Qu, J. Zhang, and Y. Lin, "Cooperative Lane Changing Strategies to Improve Traffic Operation and Safety Nearby Freeway Off-Ramps in a Connected and Automated Vehicles Environment," *IEEE Trans. Intell. Transp. Syst.*, vol. 21, no. 11, pp. 1–10, Oct. 2019, doi: 10.1109/TITS.2019.2942050.

[4] Y. Zhou and S. Ahn, "Robust local and string stability for a decentralized car following control strategy for connected automated vehicles," *Transp. Res. Part B Methodol.*, vol. 125, pp. 175–196, Jul. 2019, doi: 10.1016/j.trb.2019.05.003.

[5] Y. Zheng, M. Xu, S. Wu, and S. Wang, "Development of Connected and Automated Vehicle Platoons With Combined Spacing Policy," *IEEE Trans. Intell. Transp. Syst.*, vol. 24, no. 1, pp. 596–614, Jan. 2023, doi: 10.1109/TITS.2022.3216618.

[6] X. Shi, H. Yao, Z. Liang, and X. Li, "An empirical study on fuel consumption of commercial automated vehicles," *Transp. Res. Part Transp. Environ.*, vol. 106, p. 103253, May 2022, doi: 10.1016/j.trd.2022.103253.

[7] A. Talebpour and H. S. Mahmassani, "Influence of connected and autonomous vehicles on traffic flow stability and throughput," *Transp. Res. Part C Emerg. Technol.*, vol. 71, pp. 143–163, Oct. 2016, doi: 10.1016/j.trc.2016.07.007.

[8] Y. Zheng, Y. Zhang, X. Qu, S. Li, and B. Ran, "Developing platooning systems of connected and automated vehicles with guaranteed stability and robustness against degradation due to communication disruption," *Transp. Res. Part C Emerg. Technol.*, p. 104768, Aug. 2024, doi: 10.1016/j.trc.2024.104768.

[9] J. Lioris, R. Pedarsani, F. Y. Tascikaraoglu, and P. Varaiya, "Platoons of connected vehicles can double throughput in urban roads," *Transp. Res. Part C Emerg. Technol.*, vol. 77, pp. 292–305, Apr. 2017, doi: 10.1016/j.trc.2017.01.023.

[10] K. Dresner and P. Stone, "Multiagent traffic management: a reservation-based intersection control mechanism," *N. Y.*, p. 8, 2004.

[11] M. W. Levin, H. Fritz, and S. D. Boyles, "On Optimizing Reservation-Based Intersection Controls," *IEEE Trans. Intell. Transp. Syst.*, vol. 18, no. 3, pp. 505–515, Mar. 2017, doi: 10.1109/TITS.2016.2574948.

[12] C. Yu, Y. Feng, H. X. Liu, W. Ma, and X. Yang, "Integrated optimization of traffic signals and vehicle trajectories at isolated urban intersections," *Transp. Res. Part B Methodol.*, vol. 112, pp. 89–112, Jun. 2018, doi: 10.1016/j.trb.2018.04.007.

[13] X. Chen, M. Li, X. Lin, Y. Yin, and F. He, "Rhythmic Control of Automated Traffic—Part I: Concept and Properties at Isolated Intersections," *Transp. Sci.*, vol. 55, no. 5, pp. 969–987, Sep. 2021, doi: 10.1287/trsc.2021.1060.

[14] H. Wang, Q. Meng, S. Chen, and X. Zhang, "Competitive and cooperative behaviour analysis of connected and autonomous vehicles across unsignalised intersections: A game-theoretic approach," *Transp. Res. Part B Methodol.*, vol. 149, pp. 322–346, Jul. 2021, doi: 10.1016/j.trb.2021.05.007.

[15] A. Zhou, S. Peeta, M. Yang, and J. Wang, "Cooperative signal-free intersection control using virtual platooning and traffic flow regulation," *Transp. Res. Part C Emerg. Technol.*, vol. 138, p. 103610, May 2022, doi: 10.1016/j.trc.2022.103610.

[16] J. Ding, L. Li, H. Peng, and Y. Zhang, "A Rule-Based Cooperative Merging Strategy for Connected and Automated Vehicles," *IEEE Trans. Intell. Transp. Syst.*, vol. 21, no. 8, pp. 3436–3446, Aug. 2020, doi: 10.1109/TITS.2019.2928969.

[17] H. Xu, S. Feng, Y. Zhang, and L. Li, "A Grouping-Based Cooperative Driving Strategy for CAVs Merging Problems," *IEEE Trans. Veh. Technol.*, vol. 68, no. 6, pp. 6125–6136, Jun. 2019, doi: 10.1109/TVT.2019.2910987.

[18] S. Darbha, S. Konduri, and P. R. Pagilla, "Benefits of V2V Communication for Autonomous and Connected Vehicles," *IEEE Trans. Intell. Transp. Syst.*, vol. 20, no. 5, pp. 1954–1963, May 2019, doi: 10.1109/TITS.2018.2859765.

[19] L. Xiao, M. Wang, W. Schakel, and B. van Arem, "Unravelling effects of cooperative adaptive cruise control deactivation on traffic flow characteristics at merging bottlenecks," *Transp. Res. Part C Emerg. Technol.*, vol. 96, pp. 380–397, Nov. 2018, doi: 10.1016/j.trc.2018.10.008.

[20] A. Duret, M. Wang, and A. Ladino, "A hierarchical approach for splitting truck platoons near network discontinuities," *Transp. Res. Part B Methodol.*, vol. 132, pp. 285–302, Feb. 2020, doi: 10.1016/j.trb.2019.04.006.

[21] S. Feng, Z. Song, Z. Li, Y. Zhang, and L. Li, "Robust Platoon Control in Mixed Traffic Flow Based on Tube Model Predictive Control," *IEEE Trans. Intell. Veh.*, vol. 6, no. 4, pp. 711–722, Dec. 2021, doi: 10.1109/TIV.2021.3060626.

[22] Y. Zheng, S. Eben Li, J. Wang, D. Cao, and K. Li, "Stability and Scalability of Homogeneous Vehicular Platoon: Study on the Influence of Information Flow Topologies," *IEEE Trans. Intell. Transp. Syst.*, vol. 17, no. 1, pp. 14–26, Jan. 2016, doi: 10.1109/TITS.2015.2402153.

[23] Y. Liu, D. Yao, H. Li, and R. Lu, "Distributed Cooperative Compound Tracking Control for a Platoon of Vehicles With Adaptive NN," *IEEE Trans. Cybern.*, vol. 52, no. 7, pp. 7039–7048, Jul. 2022, doi: 10.1109/TCYB.2020.3044883.

[24] Y. Liu, D. Yao, L. Wang, and S. Lu, "Distributed Adaptive Fixed-Time Robust Platoon Control for Fully Heterogeneous Vehicles," *IEEE Trans. Syst. Man Cybern. Syst.*, vol. 53, no. 1, pp. 264–274, Jan. 2023, doi: 10.1109/TSMC.2022.3179444.

[25] Y. Wu, Z. Zuo, Y. Wang, Q. Han, and C. Hu, "Distributed Data-Driven Model Predictive Control for Heterogeneous Vehicular Platoon With Uncertain Dynamics," *IEEE Trans. Veh. Technol.*, vol. 72, no. 8, pp. 9969–9983, Aug. 2023, doi: 10.1109/TVT.2023.3262705.

[26] Q. Wang, X. (Terry) Yang, Z. Huang, and Y. Yuan, "Multi-Vehicle Trajectory Design During Cooperative Adaptive Cruise Control Platoon Formation," *Transp. Res. Rec. J. Transp. Res. Board*, vol. 2674, no. 4, pp. 30–41, Apr. 2020, doi: 10.1177/0361198120913290.

[27] Y. Bai, Y. Zhang, M. Wang, and J. Hu, "Optimal control based CACC: Problem formulation, solution, and stability analysis," in *2019 IEEE Intelligent Vehicles Symposium (IV)*, Paris, France: IEEE, Jun. 2019, pp. 7–7. doi: 10.1109/IVS.2019.8813834.

[28] M. Wang, S. P. Hoogendoorn, W. Daamen, B. van Arem, and R. Happee, "Game theoretic approach for predictive lane-changing and car-following control," *Transp. Res. Part C Emerg. Technol.*, vol. 58, pp. 73–92, Sep. 2015, doi: 10.1016/j.trc.2015.07.009.

[29] Y. Zhou, M. Wang, and S. Ahn, "Distributed model predictive control approach for cooperative car-following with guaranteed local and string stability," *Transp. Res. Part B Methodol.*, vol. 128, pp. 69–86, Oct. 2019, doi: 10.1016/j.trb.2019.07.001.

[30] M. Bashiri, H. Jafarzadeh, and C. H. Fleming, "PAIM: Platoon-based Autonomous Intersection Management," in *2018 21st International Conference on Intelligent Transportation Systems (ITSC)*, Maui, HI: IEEE, Nov. 2018, pp. 374–380. doi: 10.1109/ITSC.2018.8569782.

[31] A. Cristofoli, "New Intersection Control for Conventional and Automated Vehicles without Traffic Lights: A combination of individual control and self-regulation," Delft University of Technology, 2019.

[32] W. Zhao, R. Liu, and D. Ngoduy, "A bilevel programming model for autonomous intersection control and trajectory planning," *Transp. Transp. Sci.*, vol. 17, no. 1, pp. 34–58, Jan. 2021, doi: 10.1080/23249935.2018.1563921.

[33] B. Xu *et al.*, "Distributed conflict-free cooperation for multiple connected vehicles at unsignalized intersections," *Transp. Res. Part C Emerg. Technol.*, vol. 93, pp. 322–334, Aug. 2018, doi: 10.1016/j.trc.2018.06.004.

[34] Y. Zhang, Y. Bai, J. Hu, and M. Wang, "Chang-Hu's Optimal Motion Planning Framework for Cooperative Automation: Mathematical Formulation, Solution, and Applications," in *Transportation Research Board Annual Meeting*, 2020.

[35] D. Karaboga and B. Basturk, "On the performance of artificial bee colony (ABC) algorithm," *Appl. Soft Comput.*, vol. 8, no. 1, pp. 687–697, Jan. 2008, doi: 10.1016/j.asoc.2007.05.007.

[36] W. Y. Szeto, Y. Wu, and S. C. Ho, "An artificial bee colony algorithm for the capacitated vehicle routing problem," *Eur. J. Oper. Res.*, vol. 215, no. 1, pp. 126–135, Nov. 2011, doi: 10.1016/j.ejor.2011.06.006.

[37] X. Zhan, W. Y. Szeto, C. S. Shui, and X. (Michael) Chen, "A modified artificial bee colony algorithm for the dynamic ride-hailing sharing

problem," *Transp. Res. Part E Logist. Transp. Rev.*, vol. 150, p. 102124, Jun. 2021, doi: 10.1016/j.tre.2020.102124.

[38] C. Chen, J. Wang, Q. Xu, J. Wang, and K. Li, "Mixed platoon control of automated and human-driven vehicles at a signalized intersection: Dynamical analysis and optimal control," *Transp. Res. Part C Emerg. Technol.*, vol. 127, p. 103138, Jun. 2021, doi: 10.1016/j.trc.2021.103138.

[39] H. Liu, X. (David) Kan, S. E. Shladover, X.-Y. Lu, and R. E. Ferlis, "Modeling impacts of Cooperative Adaptive Cruise Control on mixed traffic flow in multi-lane freeway facilities," *Transp. Res. Part C Emerg. Technol.*, vol. 95, pp. 261–279, Oct. 2018, doi: 10.1016/j.trc.2018.07.027.

Dr. Yuan Zheng is currently an Assistant Professor in the School of Transportation at the Southeast University. He received his Ph.D. degree from the School of Transportation at the Southeast University, China. His interests include connected automated vehicle and traffic control, connected and automated mixed traffic flow modeling, and artificial intelligence traffic applications.

Dr. Min Xu is currently an Associate Professor in the Department of Industrial and Systems Engineering at the Hong Kong Polytechnic University. She received her Ph.D. degree from the Ph.D. degree in Transportation Engineering from National University of Singapore, Singapore. She focuses on the modeling and optimization problem in urban transportation and logistics systems with emerging technologies. She serves on editorial advisory board of Transportation Research Part C, Transportation Research Part D, and Transportation Research Part E.

Dr. Shining Wu is currently an Associate Professor in the Department of Logistics and Maritime Studies at the Hong Kong Polytechnic University. He received his Ph.D. in Industrial Engineering and Logistics Management from the Hong Kong University of Science and Technology, Hong Kong. His research interests include the sharing economy, behavioral operations management, queueing theory and its applications, and data-driven optimization.

Dr. Shuaian Wang is currently a Professor in the Department of Logistics and Maritime Studies at the Hong Kong Polytechnic University. He received his Ph.D. in Transportation Engineering from National University of Singapore, Singapore. His research interests include the big data in shipping, sustainable maritime transportation, urban transport network modeling, and green logistics and supply chain management. He is the editor or editorial advisory board member of many transportation journals including Transportation Research Part B, Transportation Research Part E.